Introduction to Neutron Radiography and Computed Tomography

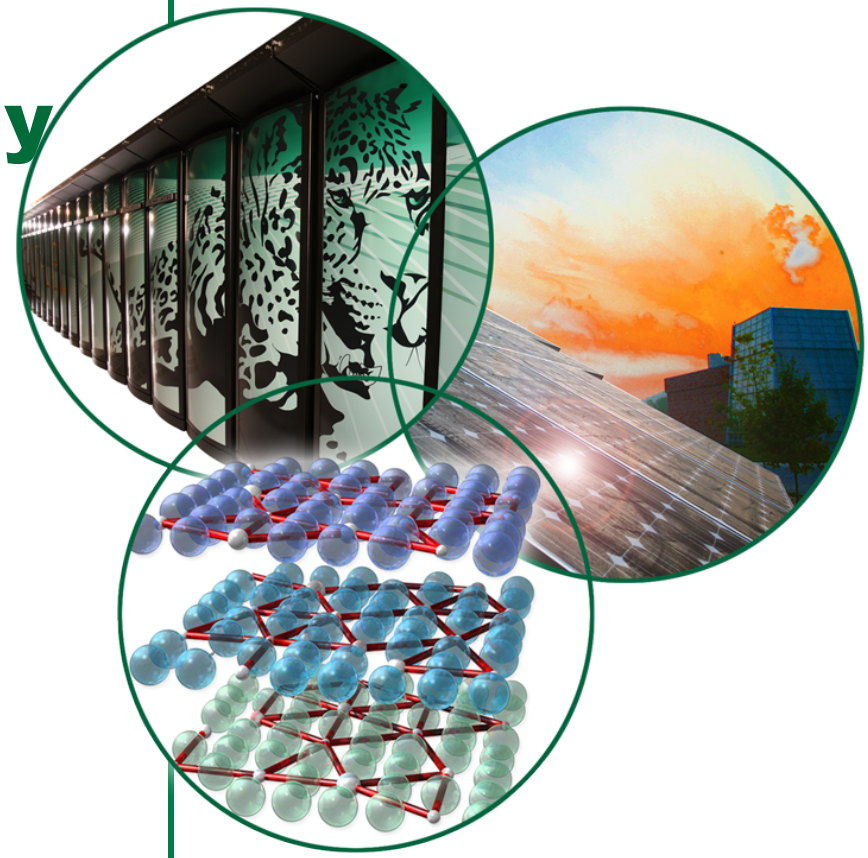

Neutron Imaging Team at CG-1D:

Hassina Bilheux, Neutron Imaging Scientist

Lou Santodonato, Scientific Associate
Jean Bilheux, User Imaging Software
Data Analysis
Barton Bailey, Engineer

NX School
June 24, 2015

U.S. DEPARTMENT OF ENERGY

OAK RIDGE NATIONAL LABORATORY
MANAGED BY UT-BATTELLE FOR THE DEPARTMENT OF ENERGY

Neutrons Measure Structure

Neutron Diffraction

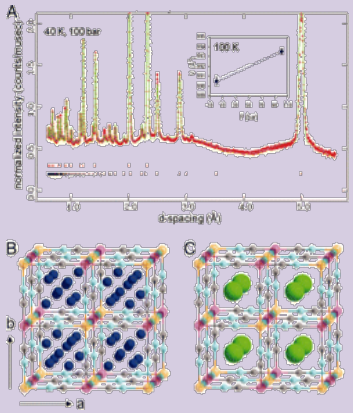

Neutron diffraction of D_2 sorption in $Cu3[Co(CN)_6]_2$

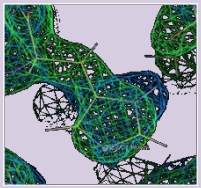

Nuclear and electronic density in enzymes

Neutron Scattering

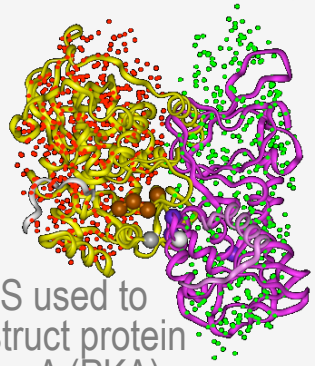

SANS used to construct protein kinase A (PKA)

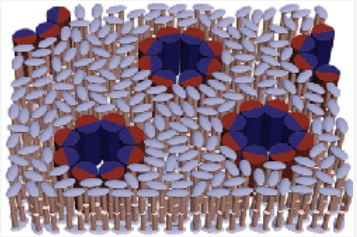

Characterization of biological membranes, colloids, porosity, etc.

Neutron Microscopy

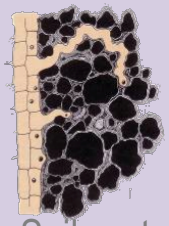

Soil-root interface (rhizosphere)

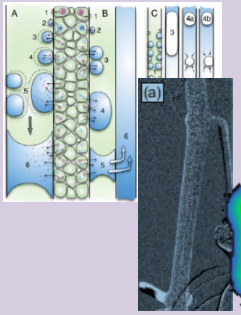

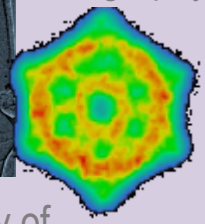

Computed tomography

In Vivo Study of Embolism Formation

Neutron Imaging

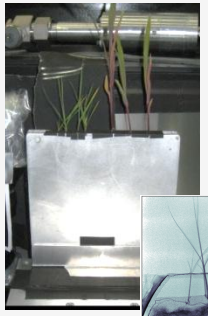

Fluid interactions in plant-groundwater systems

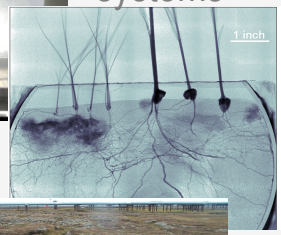

Ice/water segregation in permafrost structures

Inferred structure (indirect) — *Direct structure*

10^{-11} 10^{-9} 10^{-7} 10^{-5} 10^{-3}

Dimension (meters)

0.1Å 1.0nm 0.1μm 10.0μm 1mm

OAK RIDGE National Laboratory

Introduction

- Neutron Radiography started in the mid 1930's but only the past 30 years has it come to the forefront of non-destructive testing.
- State-of-the-art facilities in the U.S., Europe, Asia, Africa, etc.
- World conferences and workshops being held regularly
- Growing worldwide user community

Neutron classification	Energy (meV)	Velocity (m/s)	λ (nm)
Ultra-cold	0.00025	6.9	57
Cold	1	437	0.9
Thermal	25	2187	0.18
Epithermal	1000	13,832	0.029

D. L. Price and K. Sköld in N*eutron Scattering,* Academic Press, Orlando, Fl., 1986), Vol. A.

Neutron sensitivity

Neutron Radiograph of camera

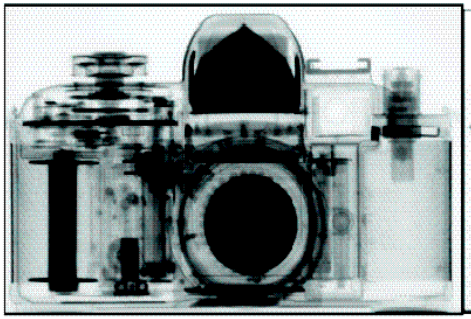

X-ray Radiograph of camera

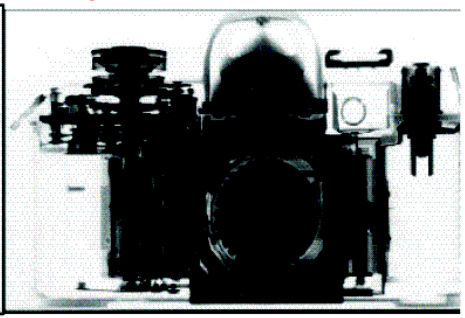

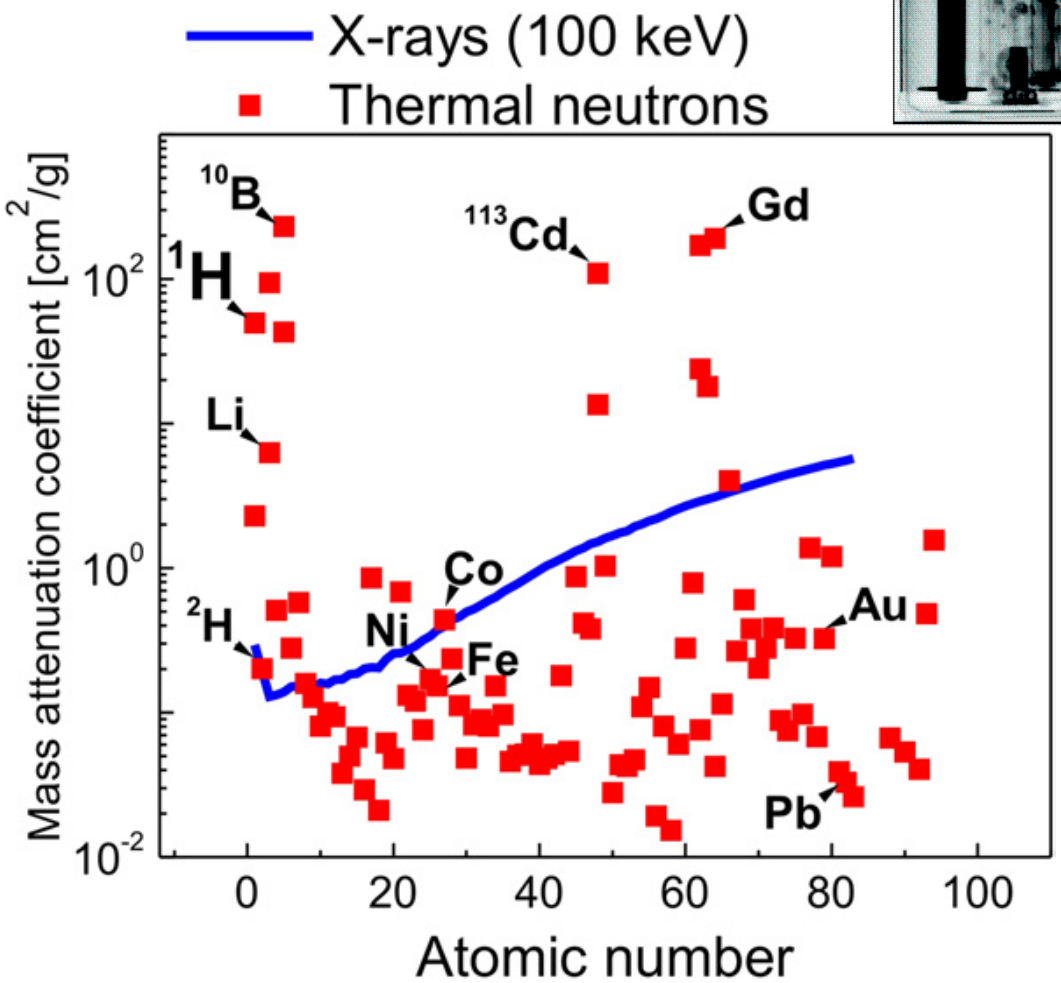

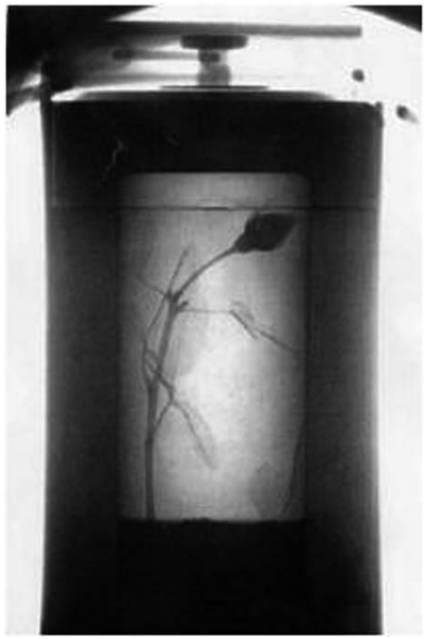

Neutron Radiograph of Rose in Lead Flask

Courtesy of E. Lehmann,PSI

*[M. Strobl et al., J. Phys. D: Appl. Phys. **42** (2009) 243001]*

Managed by UT-Battelle
for the U.S. Department of Energy

What is imaging?

- **Imaging is the visual representation of an object:** photography, cinematography, medical imaging, X-ray imaging, thermal imaging, molecular imaging, neutron imaging, etc.

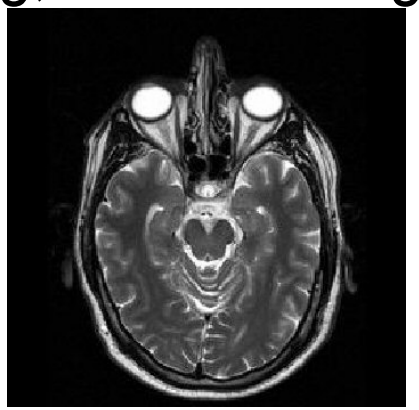

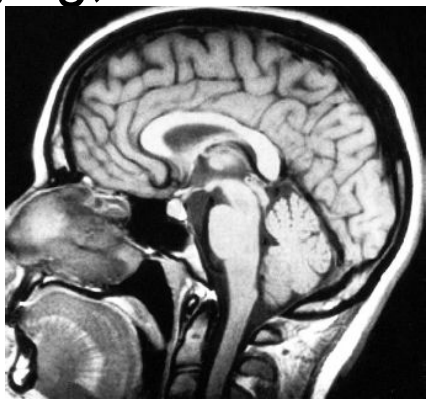

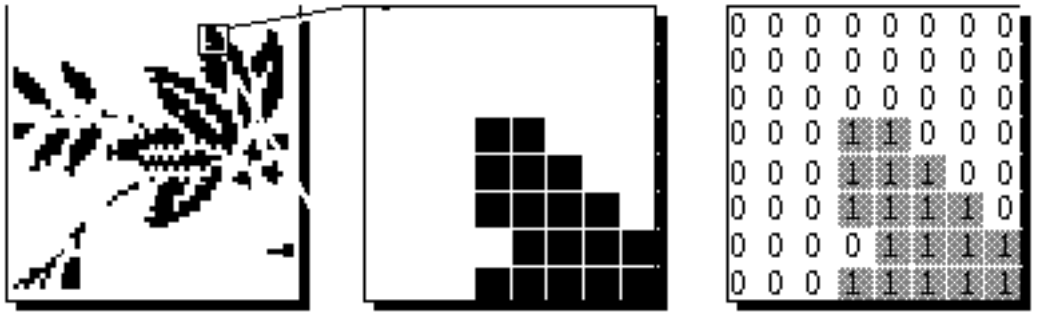

- **Digital Imaging is a field of computer science covering images that can be stored on a computer as *bit-mapped* images**

Early neutron imaging measurements

- **Neutron Imaging started in the mid 1930's but only during the past 30 years has it come to the forefront of non-destructive testing**

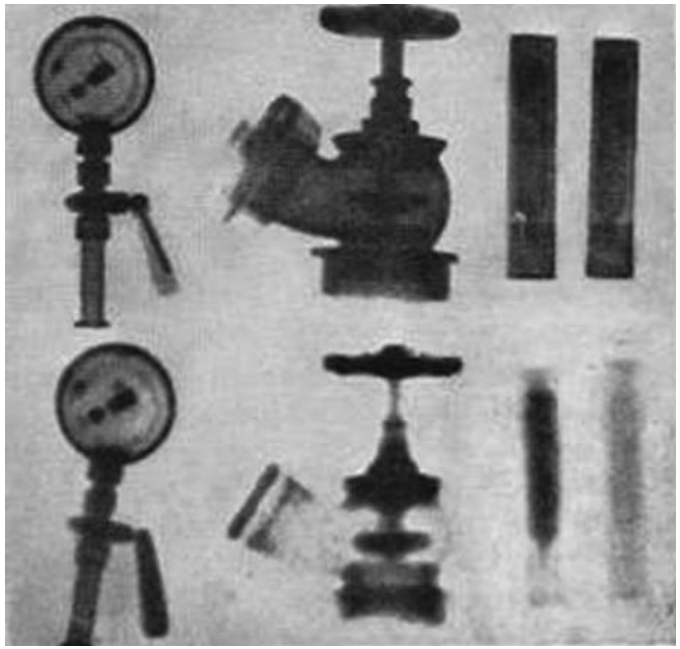

Discovery of neutron in 1932 by Chadwick

First neutron radiograph in 1935

Left to right: Pressure gauge with metal backplate; fire hydrant and test tubes filled with H2O
and D2O imaged with gamma-rays (top) and neutrons (bottom)
[Kallman and Kuhn, Research 1, 254 (1947)]

- **World class dedicated imaging user facilities such as NIST, PSI, HZB, FRM-II and at many worldwide universities**
- **World conferences and workshops being held regularly**
- **Growing worldwide user community**

Multiple scattering and low detector spatial resolution

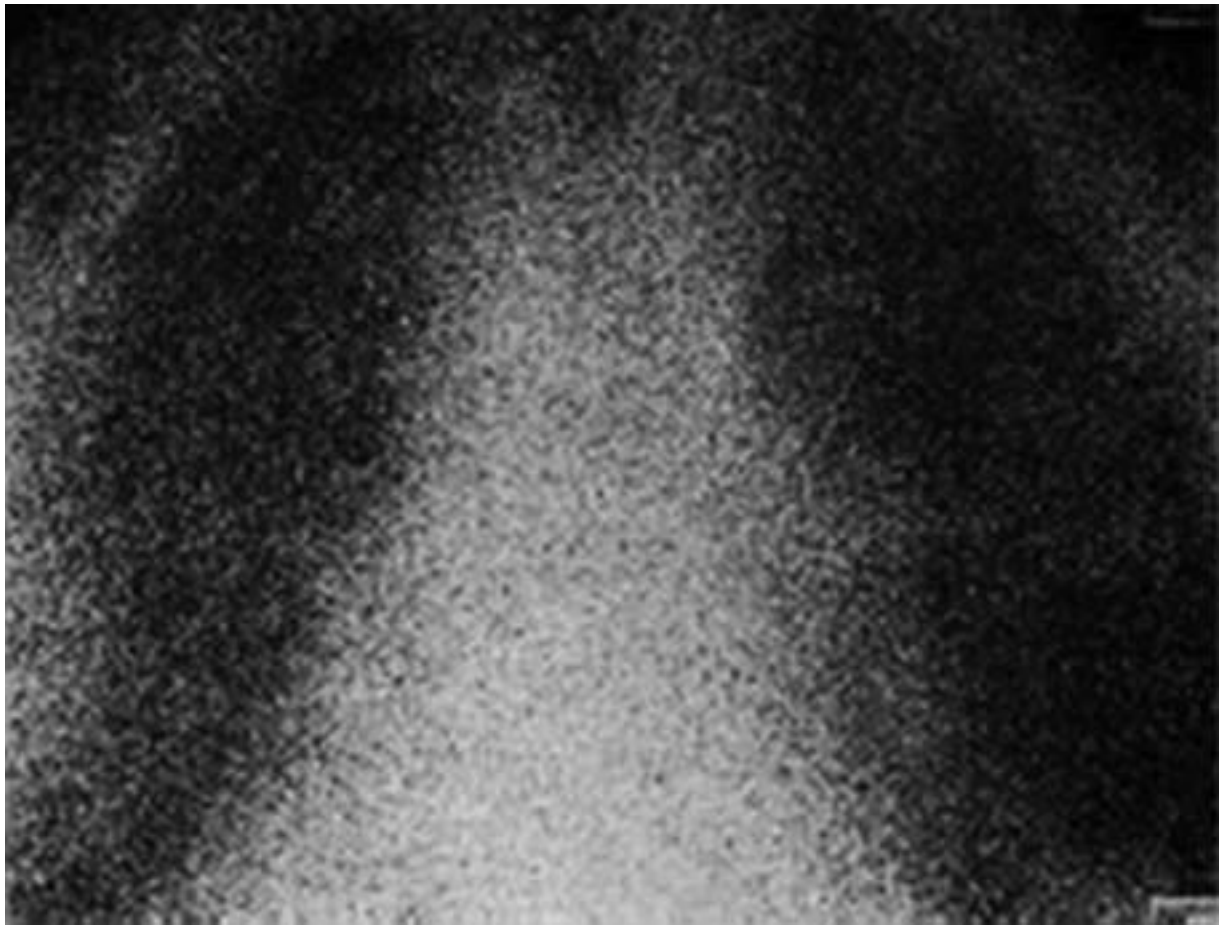

[J. Anderson et al., Br. J. Radiol. 37, 957 (1964)]

Today: Comparison microscopy/microCT and neutron radiography

Microscope

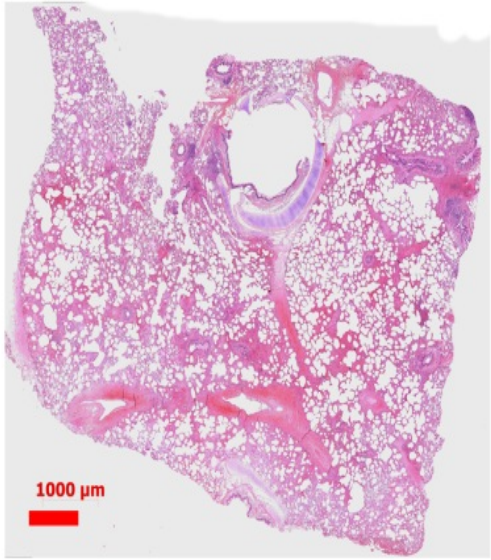

microCT

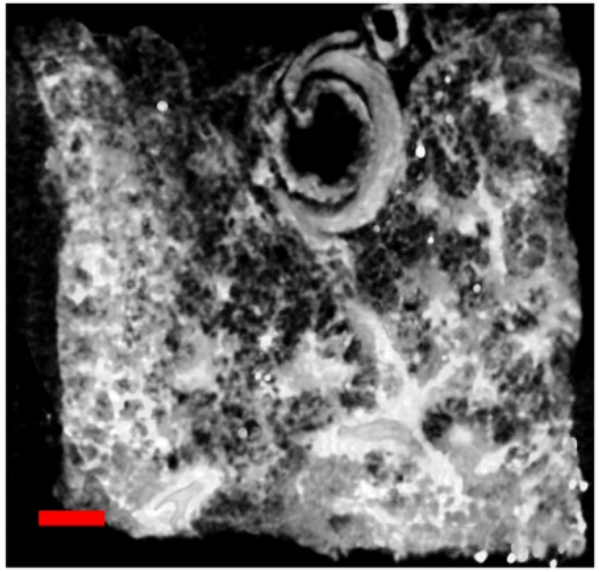

Neutron

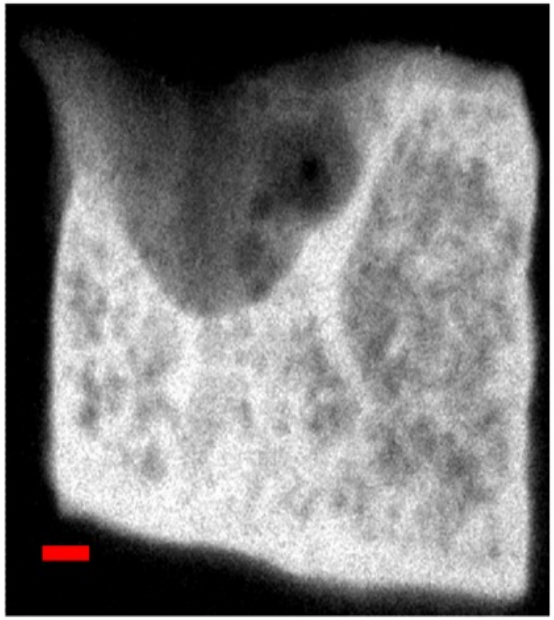

- **92% of the pixel intensities agreement between histological and neutron**

Watkin, K. et al., Neutron Imaging and Applications, Springer, 2009.

OAK RIDGE National Laboratory

Basics of Neutron imaging

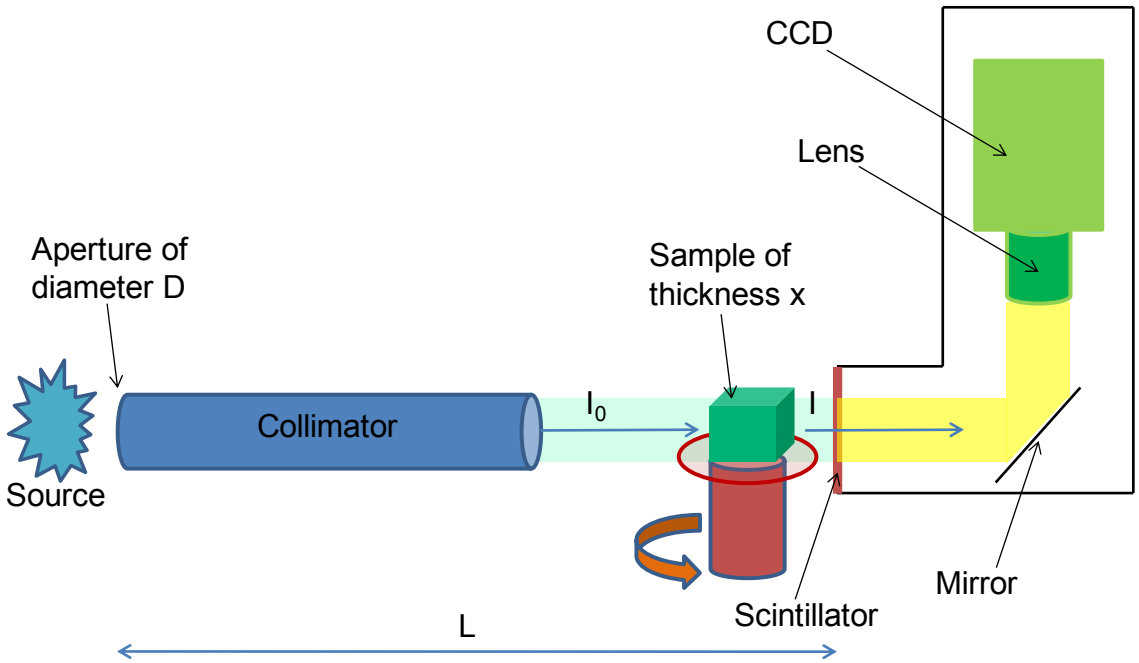

Photograph

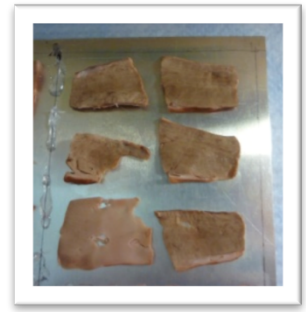

Neutron Radiograph

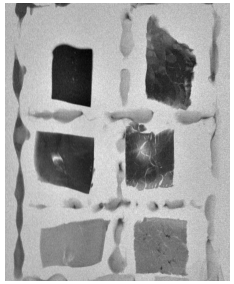

Beam attenuation caused by a **homogeneous uniformly** thick sample composed of a **single isotope** is given by

$$I(\lambda) = I_0(\lambda)e^{-\mu(\lambda)x}$$

$$\mu(\lambda) = \sigma_t(\lambda)\frac{\rho N_A}{M}$$

$\sigma_t(\lambda)$ = scattering and absorption

μ is the attenuation coefficient and Δx is the thickness of the sample

$\sigma_t(\lambda)$ is the material's total cross section for neutrons, ρ is its density, N_A is Avogadro's number, and M is the molar mass.

Detection of "imaging" neutrons

- Scintillator-based techniques such as $^{6}Li(n,\alpha)\ ^{3}H$
  - Good signal-to-noise (SNR) ratio
  - Large Field Of View (FOV) and 0.01 to hundreds of seconds images
  - BUT spatial resolution limited by the dissipation of particles
  - Can take a lot of neutron flux!

1,1	1,2	1,3	…	…	1, ny
2,1	2,2	2,3	…	…	2, ny
3,1	3,2	…	…	…	3, ny
…	…	…	…	…	…, nx
nx, 1	nx, 2	nx, 3	…	…	nx, ny

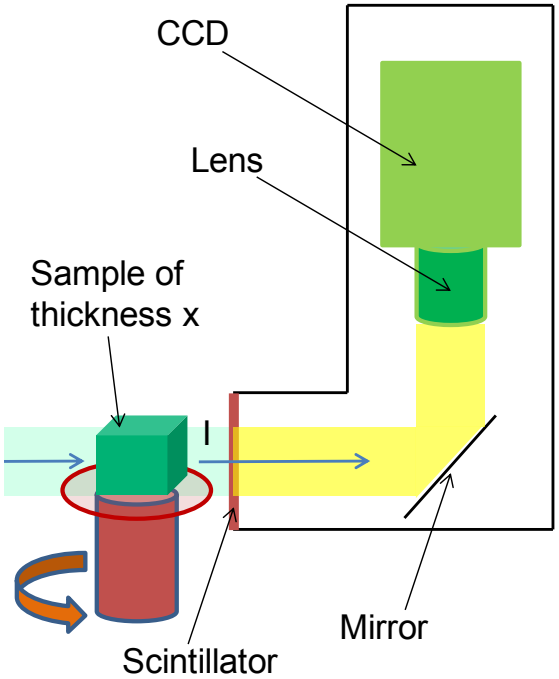

Each pixel is coded using n-bit.
16-bit = pixel value is between 0 and 65535

Detection of “imaging” neutrons (cont’d)

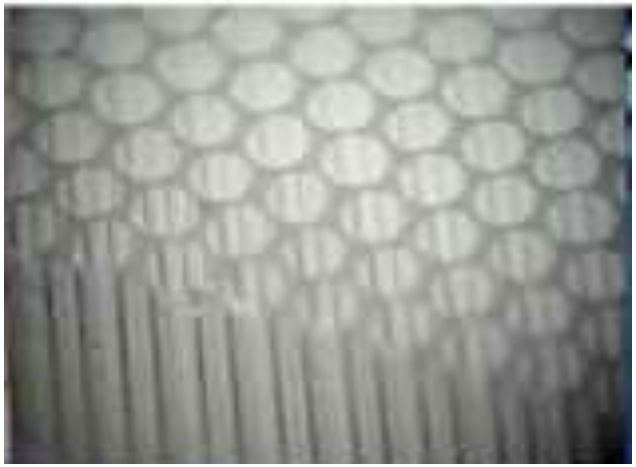

- Pixelated detectors
  - Micro-Channel Plate (MCP)
  - In the direct path of the beam
  - Limited FOV for high spatial resolution MCPs
    - 2.8 cm x 2.8 cm at ~ 15 microns
  - Encodes events at x, y position and time of arrival, at high temporal resolution ~ 1 MHz
  - Detection efficiency has improved for both cold (~70%) and thermal (~50%) energy range
  - Absence of readout noise
  - Not as gamma sensitive
  - Becoming commercial
  - BUT: works in relatively low-signal beam!

OAK RIDGE National Laboratory

Example: Cu, Zn and Al

Compound	Abs. Coeff. [Å^{-2}]	Inc. Coeff. [Å^{-1}]
Cu (100%)	1.78E-09	4.65E-10
Al (100%)	7.75E-11	4.94E-12
Zn (100%)	4.06E-10	5.06E-11

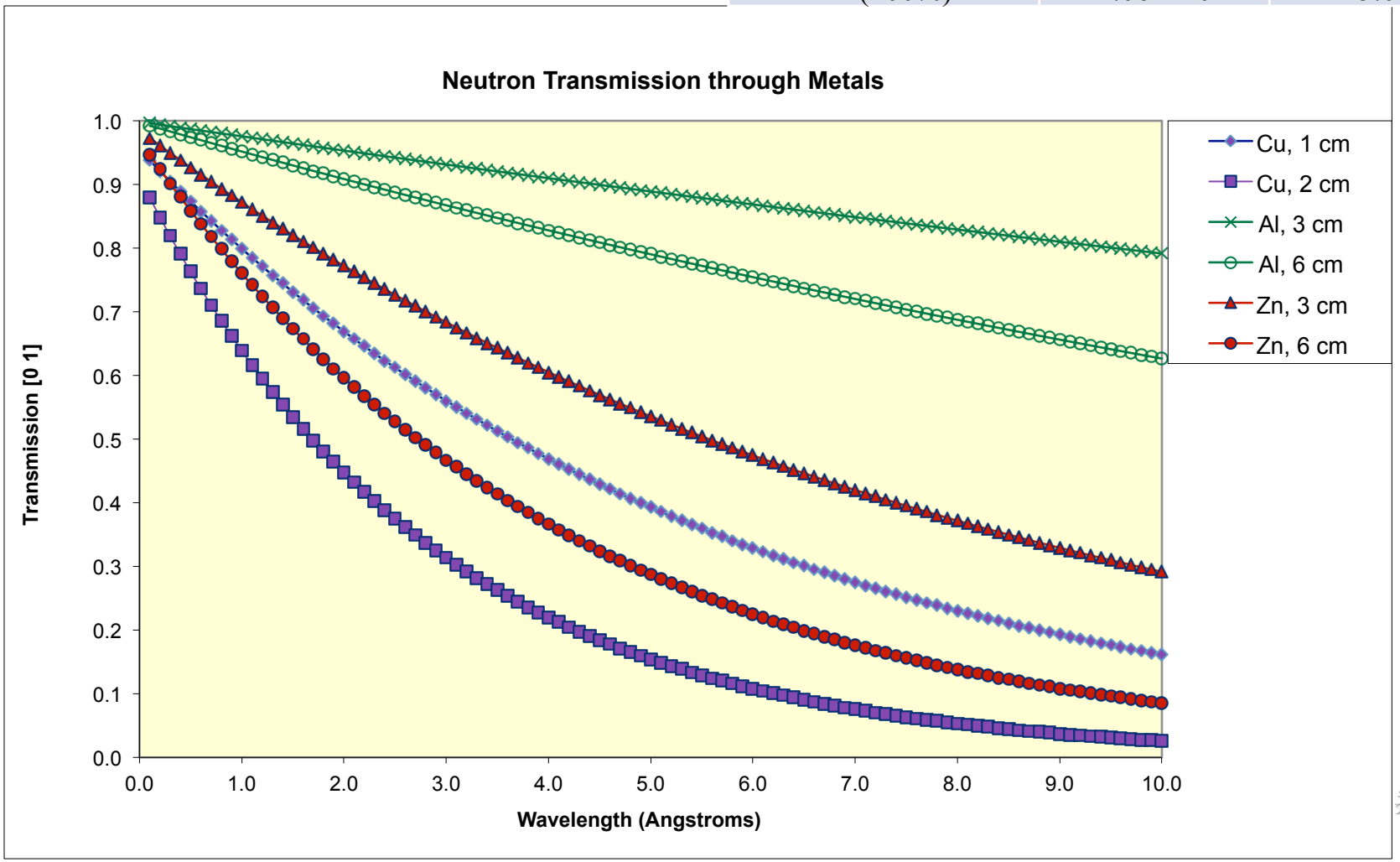

OAK RIDGE National Laboratory

CG-1D Neutron Imaging Facility

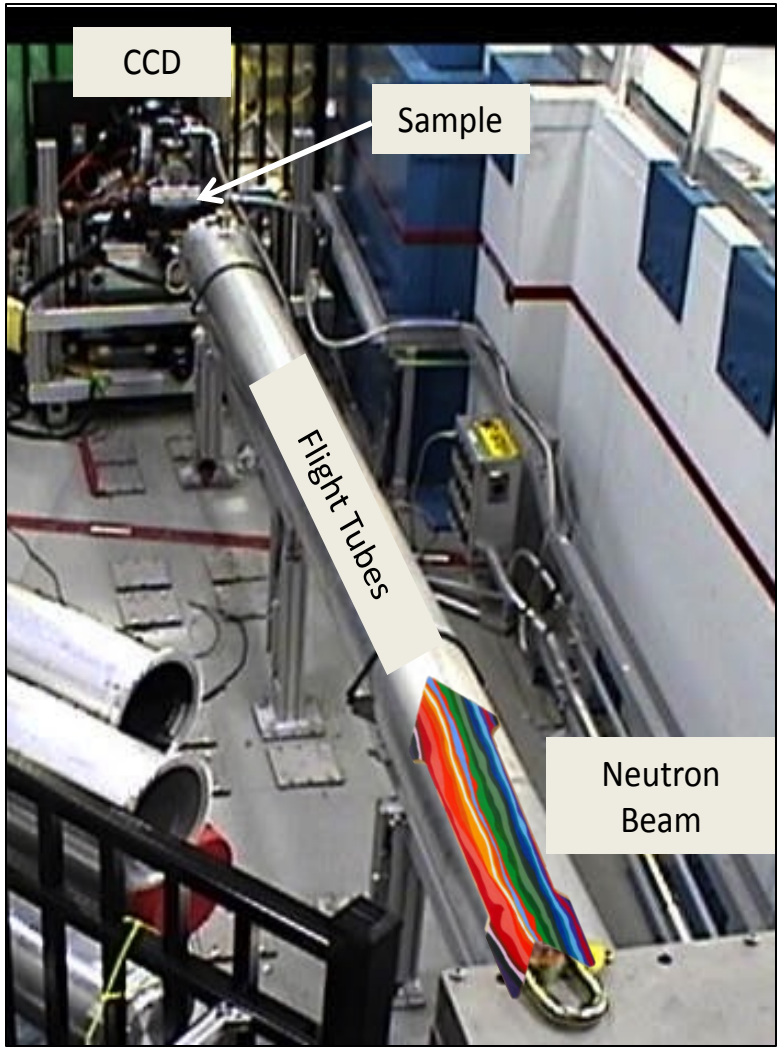

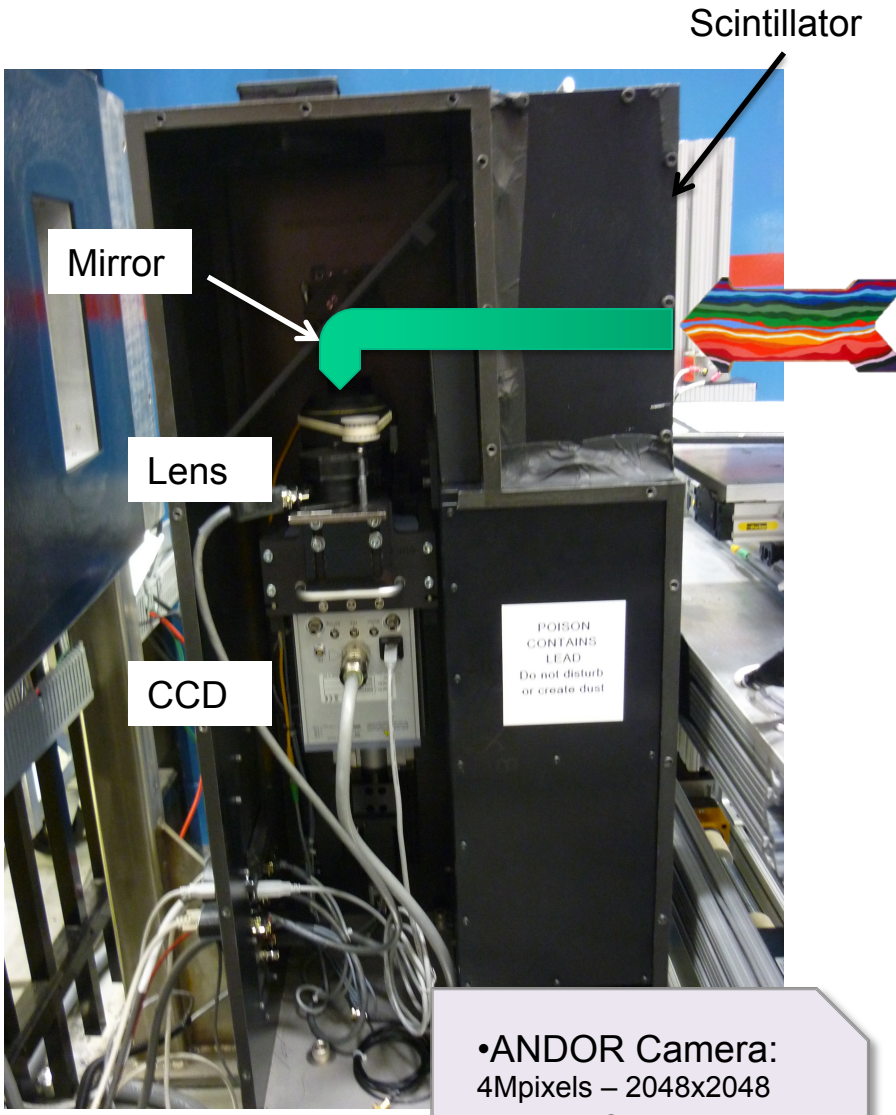

- ANDOR Camera:
  4Mpixels – 2048x2048
- Field of view:
  7.4x7.4cm^2 at 100 microns
- Quantum Efficiency:
  95%

HFIR Neutron Imaging Facility (CG-1D)

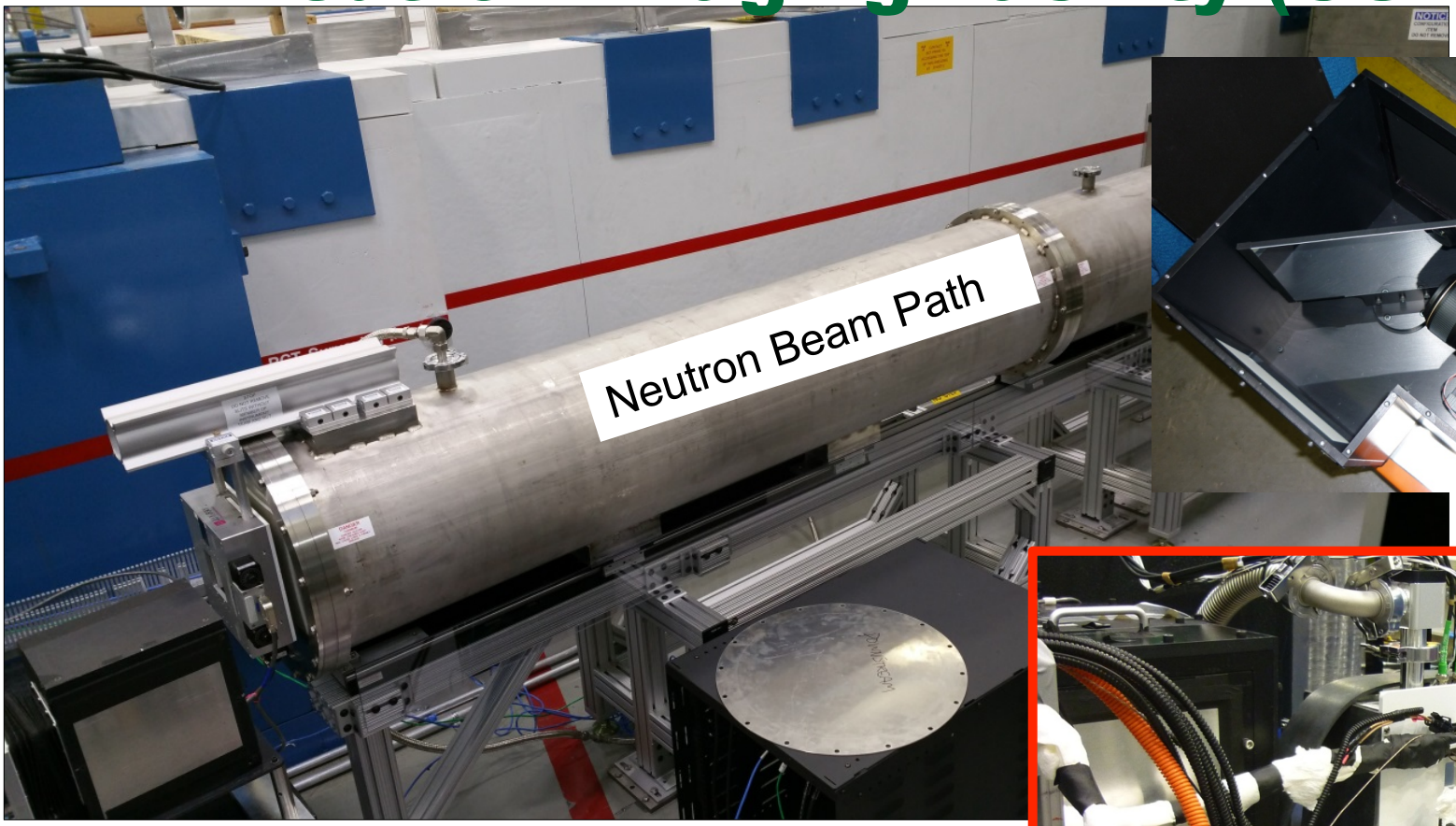

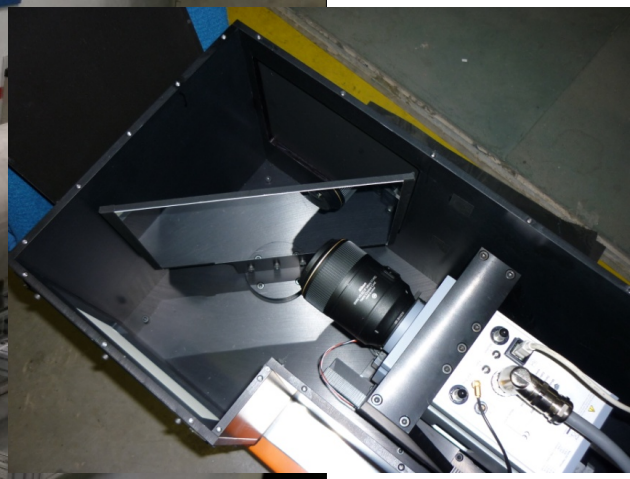

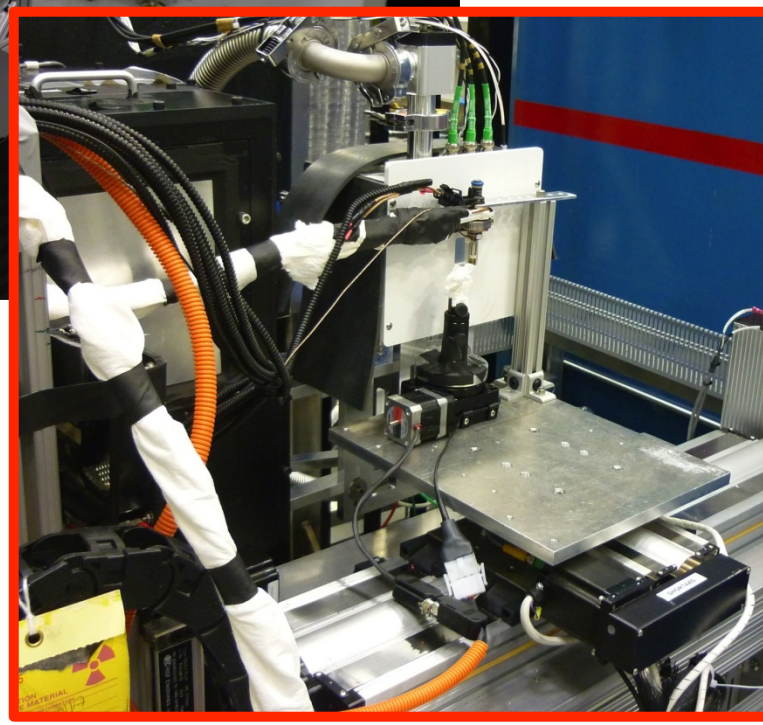

Detector capability/spatial resolution:
ANDOR® CCD Detector ~ 100 microns
sCMOS ~ 50 microns, 100 fps
MCP(*) ~ 100 microns (and ~ 15 microns in centroiding mode), or microsecond time frames

(*) In Collaboration with Prof. Anton Tremsin, UC-Berkeley

Neutron imaging supports applied research with academia, industry and government agencies

Cummins
Mack TRUCKS
Honeywell
JOHN DEERE
DETROIT DIESEL
MODINE APPLIED THERMAL INNOVATION
DELPHI
Ford
United Technologies
GM
MARS incorporated
DURACELL
NASA
DARPA
THE UNIVERSITY OF MEMPHIS
THE UNIVERSITY OF CALIFORNIA BERKELEY 1868
UAH THE UNIVERSITY ABAMA IN TSVILLE
PRINCETON UNIVERSITY
THE UNIVERSI TENNESSEE KNOXVILLE
UB UNIVERSITÉ DE BOURGOGNE
UTPA THE UNIVERSITY OF TEXAS-PAN AMERICAN
VANDERBILT
GT
NIJ National Institute of Justice
THE UNIVERSITY OF UTAH
OAK RIDGE National Laboratory

The CG-1D detector suite and respective common applications

Type of detector	Largest field-of-view (cm^2)	Effective pixel size where the image is formed (microns)	Corresponding spatial resolution (microns)	Maximum Dynamic resolution (no pixel binning)	Dynamic range (bit)	Applications
CCD	7.4 x 7.4	36	~100	1 image/ second	16	Additive Manufacturing (AM), Energy, Aerospace, Transportation Research, Geosciences, Biology, Botanical, Archeology, Medical, Food Science
sCMOS	3.3 x 2.8	13	< 100	100 images/ second for 4 sec max (**)	16	AM, Geosciences, Petroleum, Food Science
MCP (*)	2.8 x 2.8	55	~100	1 million images/ second	14	Transportation Research, AM, Energy, Aerospace, Biology, Geosciences, Petroleum, Botanical, Food Science
	2.8 x 2.8	10	~ 15	1 image/ 8 hours	14	Biology, Botanical, Medical

(*) The MCP detector has two modes of operation: the high time resolution and the high spatial resolution options, respectively.
(**) When binning pixels or working at lower frame rate, the limit is the 5 TB storage on the sCMOS server (each image is 10 MB). We can thus collect thousands of images.

OAK RIDGE National Laboratory

CG-1D polychromatic beam

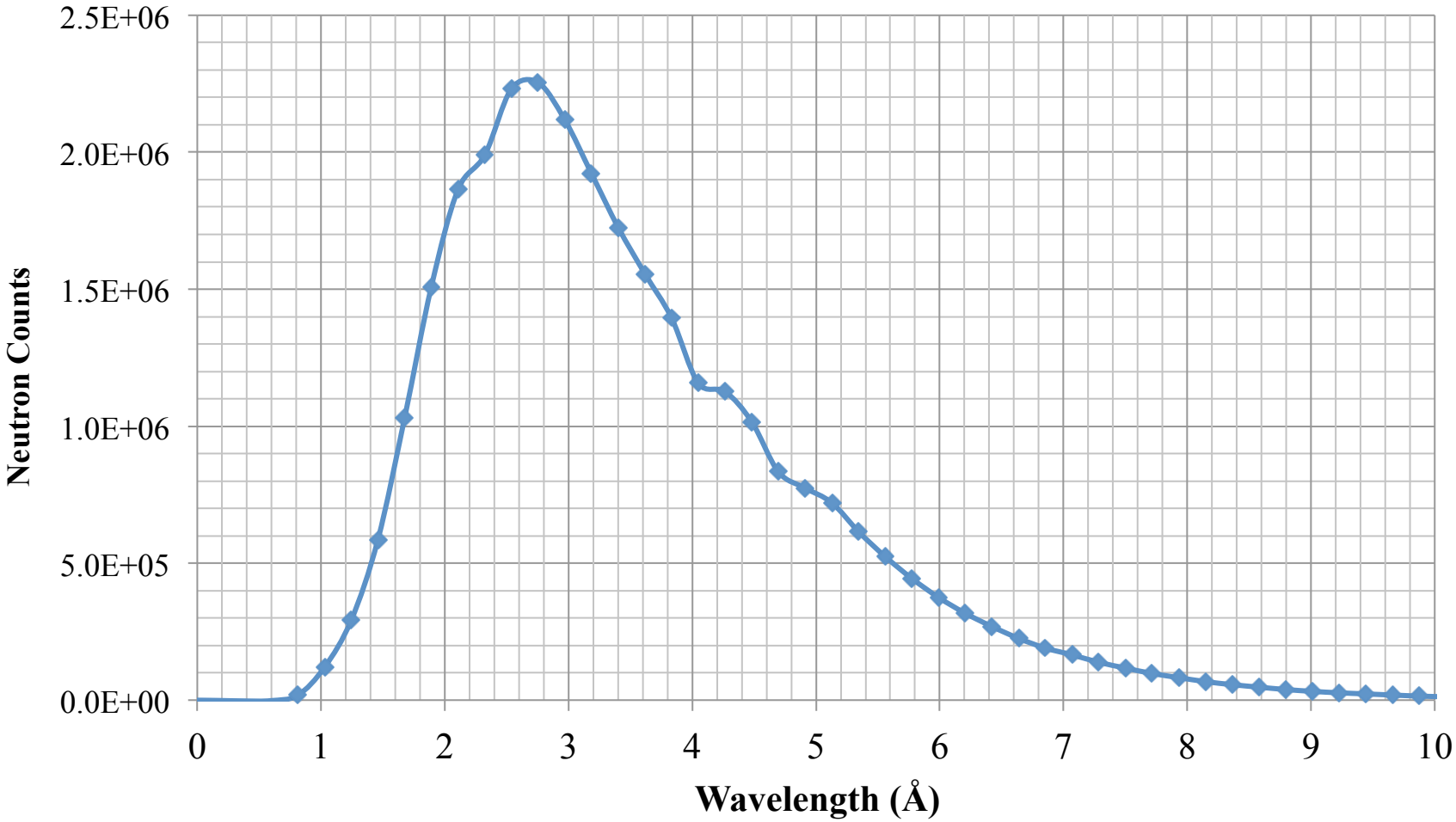

CG-1D spectrum measured with the MCP detector at a flight path distance of approximately 5.5 m, with the chopper running at a frequency 40 Hz and an 5 mm aperture. *Kang M. et al., Nuclear Instruments and Methods, 708, 2013]*

Use of Diffusers

- 1 cm thick Graphite Powder (4 to 10 microns)

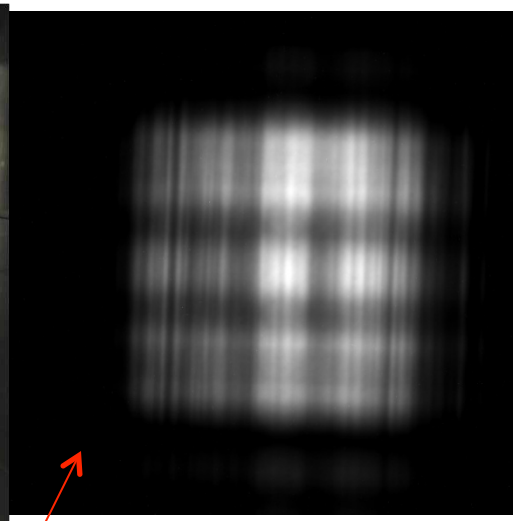

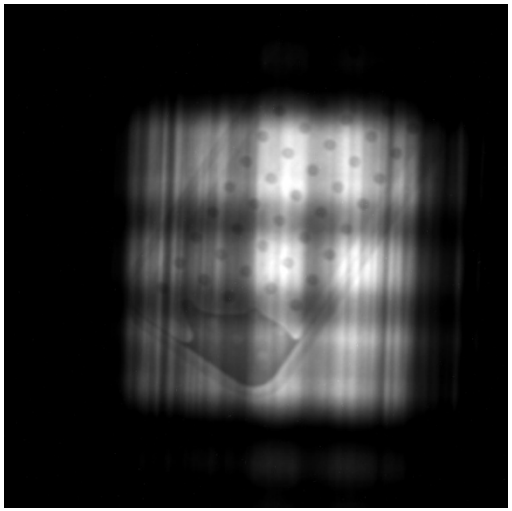

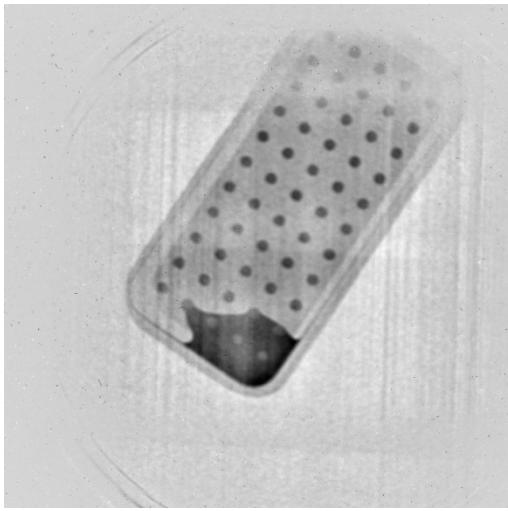

Open Beam | Heat Pipe Sample | Reduced Image

Without diffuser

With diffuser

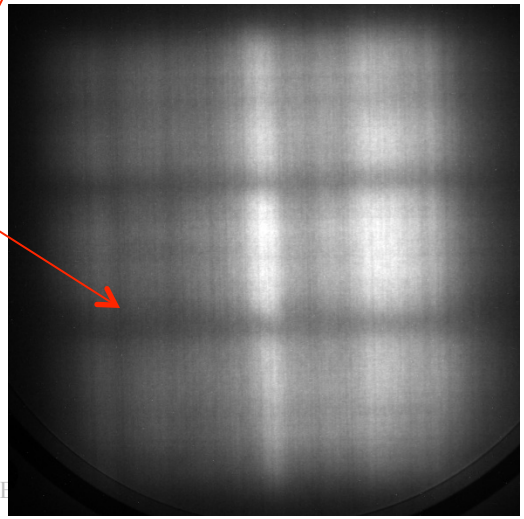

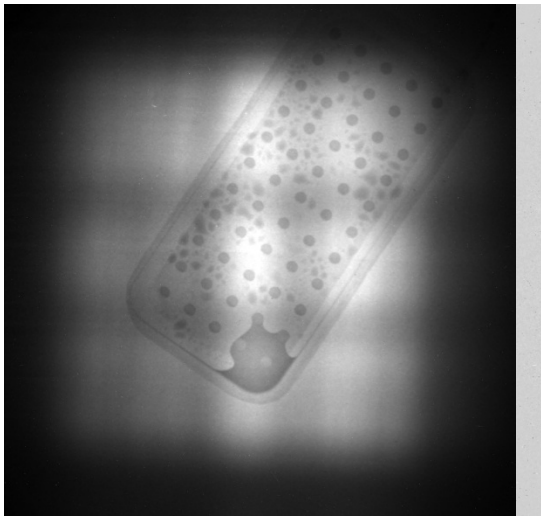

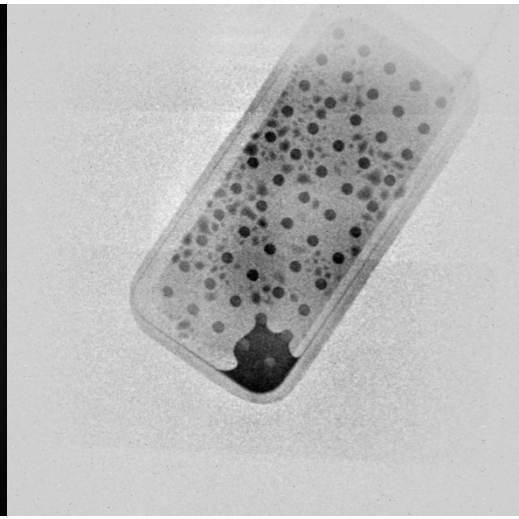

Conventional Neutron Imaging Techniques at steady-state sources

- Radiography (available at CG-1D)
- Tomography (available at CG-1D)
- Phase Contrast Imaging
- Polarized Neutron Imaging
- Stroboscopic Imaging
- Imaging of processes that happen fast
- Energy selective techniques possible with double-monochromator configuration

OAK RIDGE National Laboratory

Data Normalization for Imaging

- **2D – Radiography**
  - **Normalization**

$$I_N(i,j) = \frac{I(i,j) - DF(i,j)}{OB(i,j) - DF(i,j)}$$

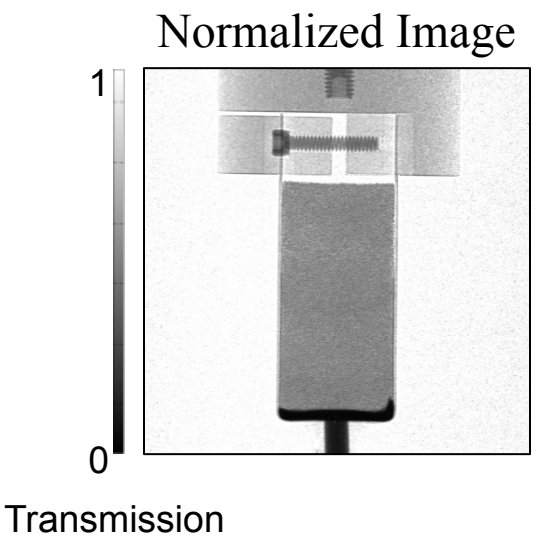

=

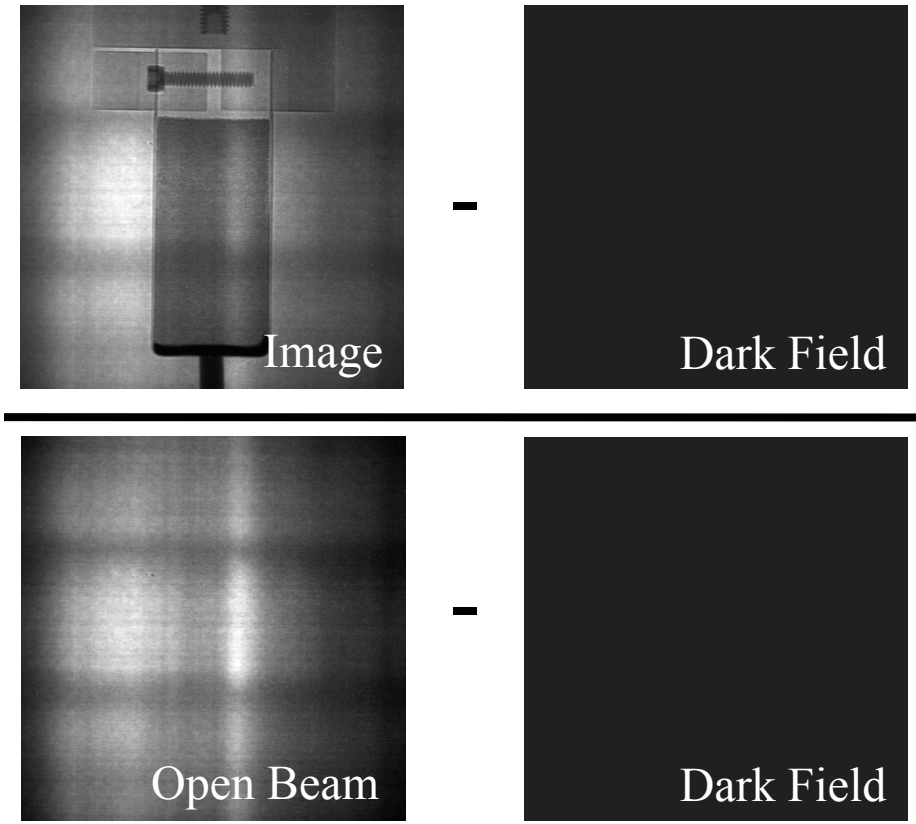

Sample stage for nCT

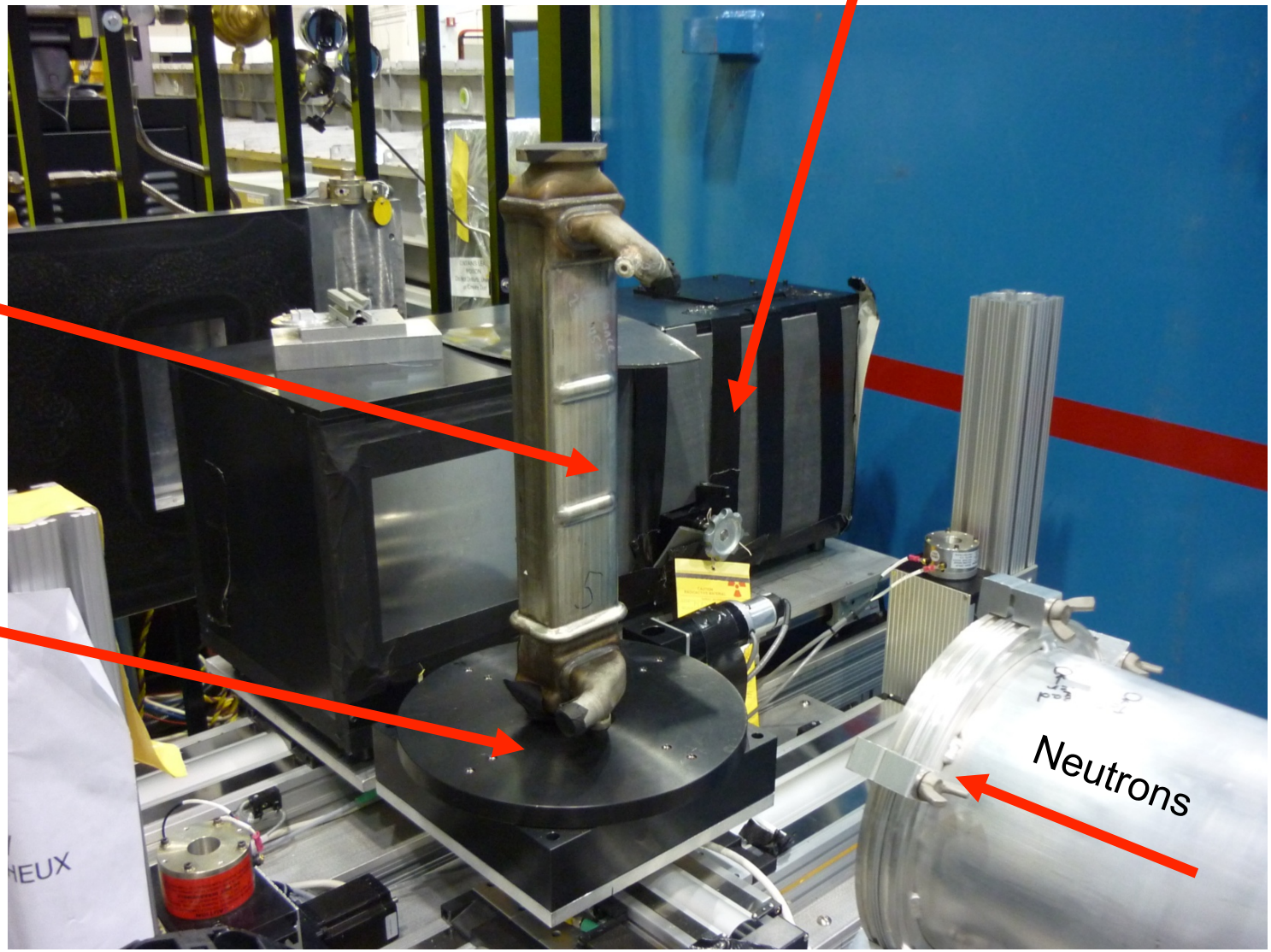

Computed/Computerized Tomography (FBP)

– **Filtered back projection method**

Raw Data: 2048x2048 pixels, 721 projections — **Normalized Data:** 2048x2048 pixels, 721 projections — **Sinograms:** 2048x721 pixels, 2048 files — **Slices:** 2048x2048 pixels, 2048 slices → **3D reconstruction: 2048x2048x2048 voxels**

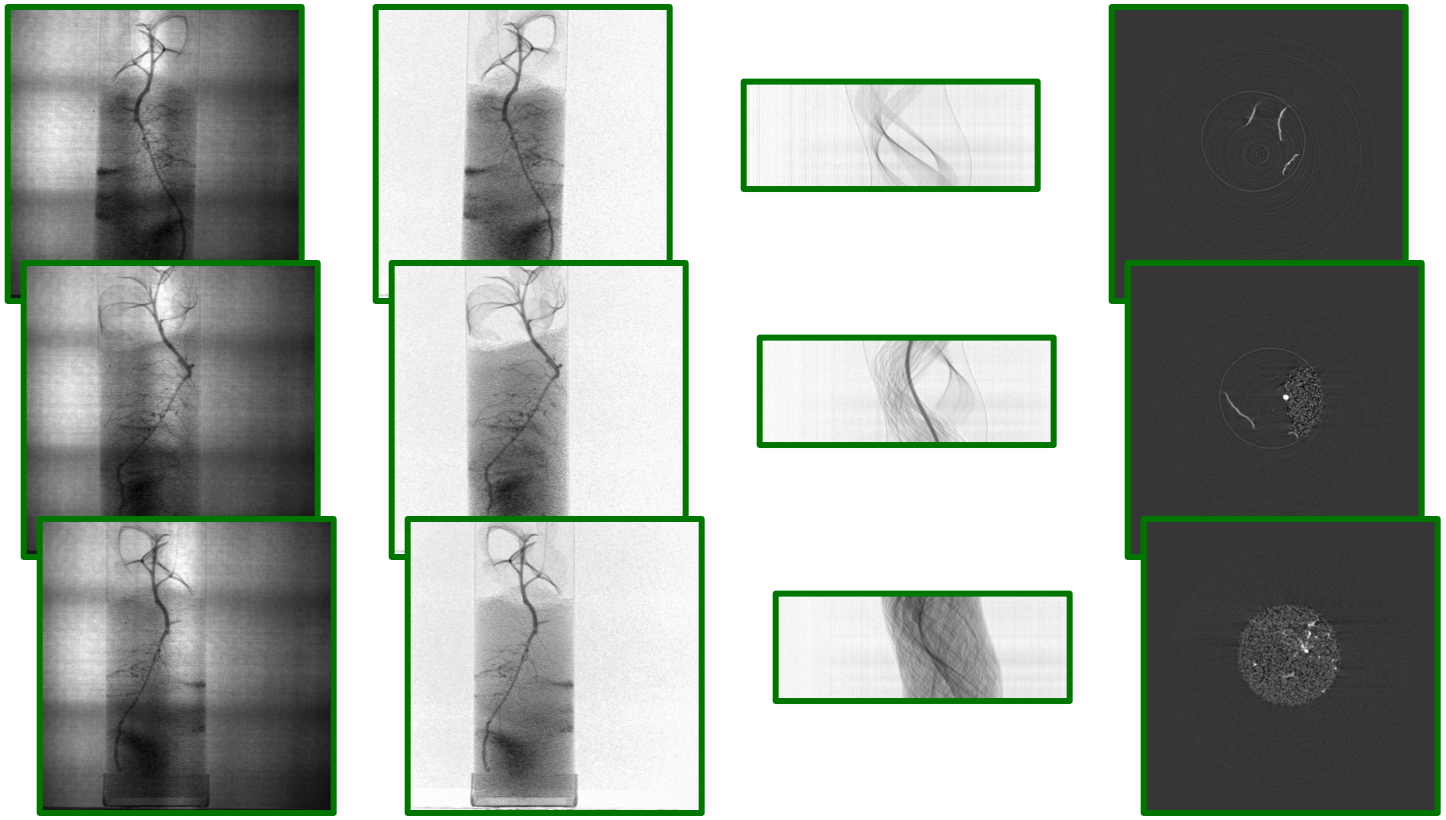

~700 Counts ~20700 | 0 Transmission 1 | 0 Transmission 1 | 0 Attenuation ∞

OAK RIDGE National Laboratory

Computed/Computerized Tomography (CT)

- Several techniques:
  - Filtered Back Projection
    - Radon transform
    - Works well with high signal to noise ration measurements
    - Easy-to-use commercial, semi-automated software available
    - Quick
  - Iterative Reconstruction
    - Direct approach
    - Less artifacts
    - Can reconstruct incomplete data
    - High computation time

Neutron Imaging Techniques at pulsed sources

- Energy-selective (or Time-of-Flight) imaging
  - Contrast enhancement
  - Bragg edge
- Energy resonance imaging
- Stroboscopic imaging
  - SNS has a natural clock
- Neutron Imaging at energies not accessible at reactor facilities
  - Mainly bio-medical applications

OAK RIDGE National Laboratory

Neutron imaging techniques

- Radiography
- Computed tomography
- Bragg edge imaging
- Neutron phase imaging
- Stroboscopic imaging
- Neutron Stimulated Computed Emission Tomography or NSECT
- Polarized imaging
- Dark field imaging
- Energy resonance imaging

Bragg Edge Imaging

- At reactors:
  - monochromatic beams
  - Scintillator-based detection adequate
- At spallation sources:
  - Time-stamping of neutrons
  - Pixelated detectors such as MCPs required for time measurements

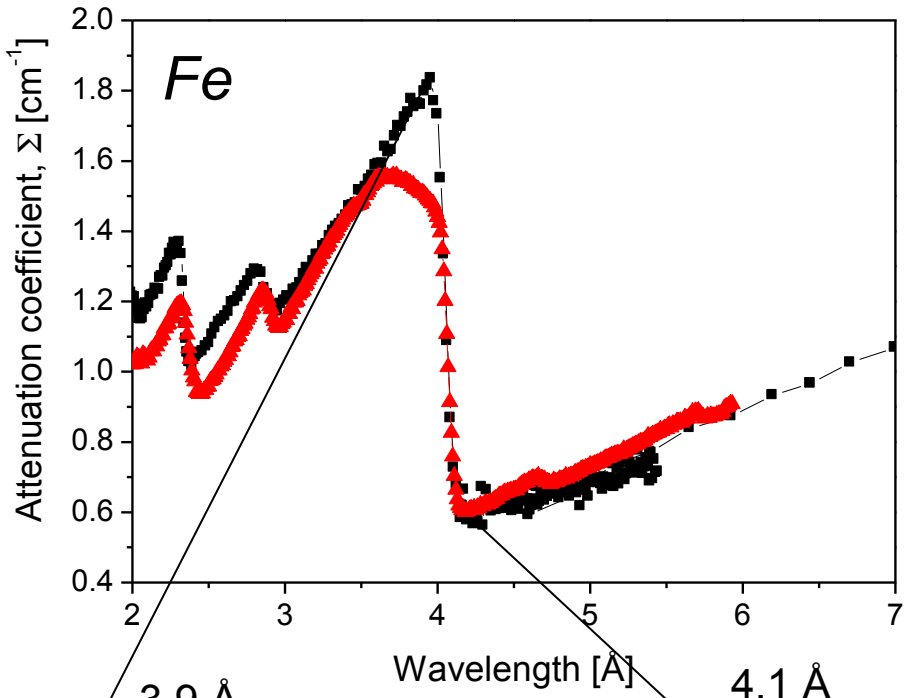

3.9 Å

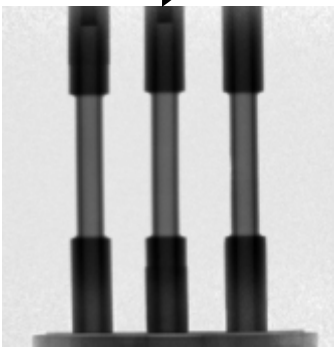

4.1 Å

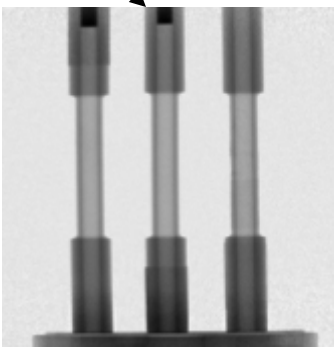

1 cm

Courtesy of Prof. D. Penumadu, UTK and N. Kardjilov, HZB

Bragg Edge Imaging

- **Strain mapping od steel screw**

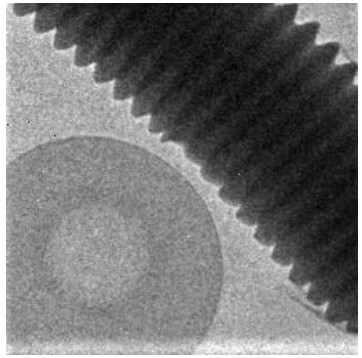

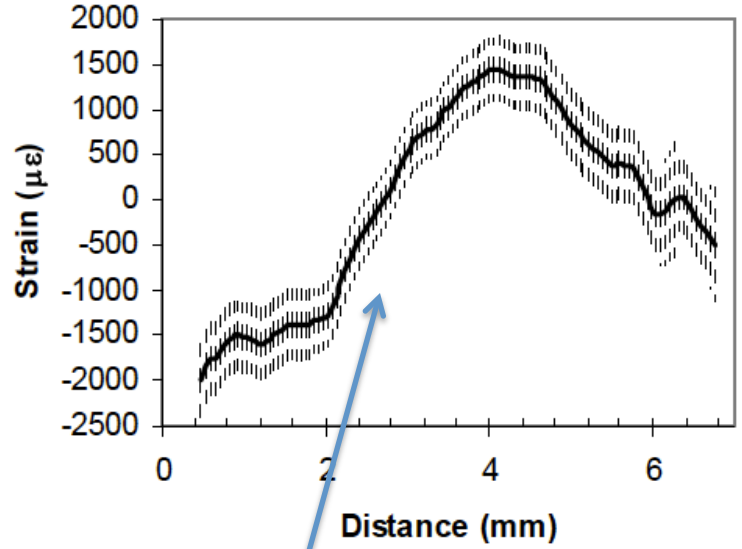

5 min exposure, 1 μs time res.

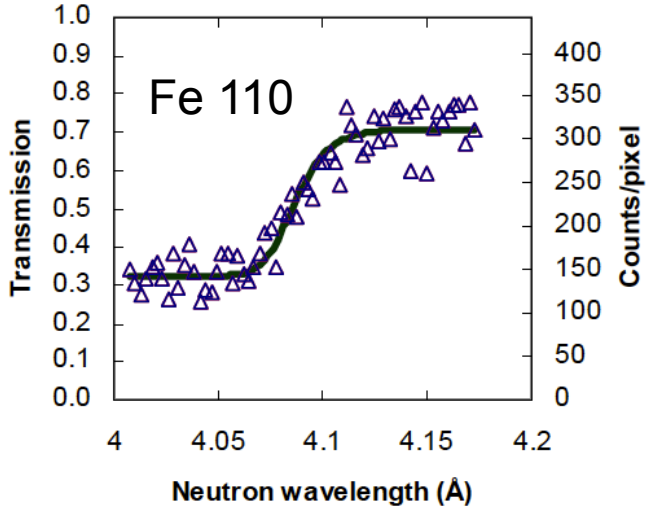

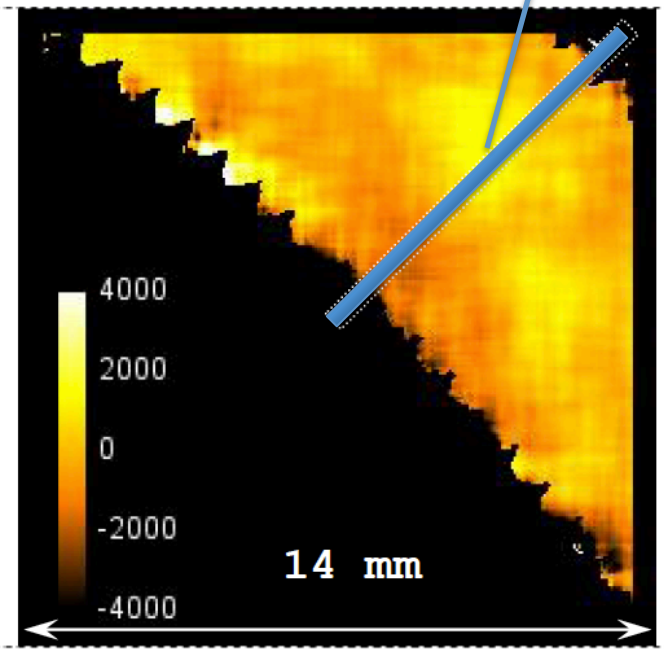

Strain map image of the steel screw. Strain values in μstrain

Tremsin et al., Journal of Physics, Conference Series 251 (2010) 012069

Managed by UT-Battelle
for the U.S. Department of Energy

Bragg Edge Imaging

- **Texture mapping**

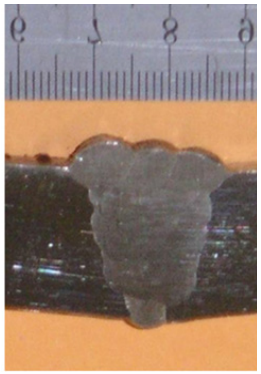

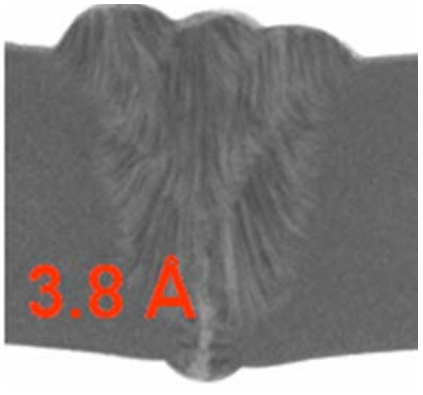

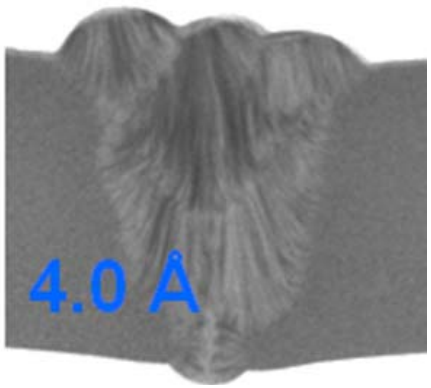

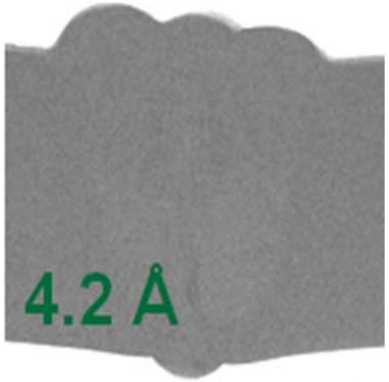

Bragg reflected neutrons result in narrow dips in the actual transmission at precise wavelengths specified by Bragg's law:

$$\lambda_{hkl} = 2d_{hkl} \sin\theta_{hkl}$$

where d_{hkl} is the interplanar distance for the (*hkl*) planes and θ_{hkl} are the Bragg angles θ_{hkl} depends on the relative orientation of the crystal lattice to the neutron beam.

At λ_{hkl}, creation of map of the number of crystals having any of their (*hkl*) directions making an angle, β_{hkl}, with the incident beam given by:

$$\beta_{hkl} = (\pi/2) - \arcsin(\lambda_{hkl} / 2d_{hkl})$$

Kockelmann et al., NIM A, Vol. 578 (2007) 421.

Propagation-based Neutron Phase Imaging

- Source needs to be spatially coherent (i.e. small pinhole and long pinhole-detector distances)
- Flux is low (up to 98% of flux is sacrificed, several hours to days for one radiograph)

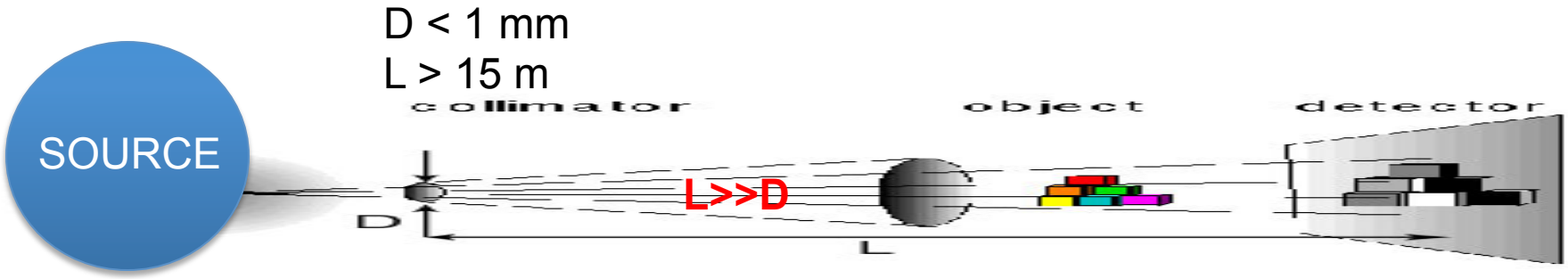

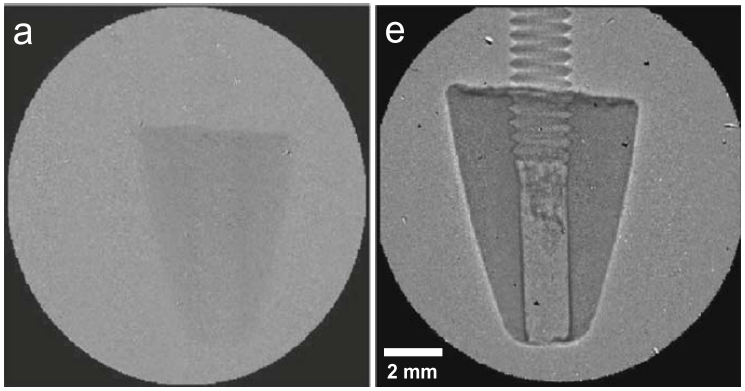

*(a) Neutron attenuation radiograph (e) and phase contrast radiograph of a lead sinker mounted on an Al screw. [B. Schillinger et al., **Mat. Trans. Proc.** (2006) 61]*

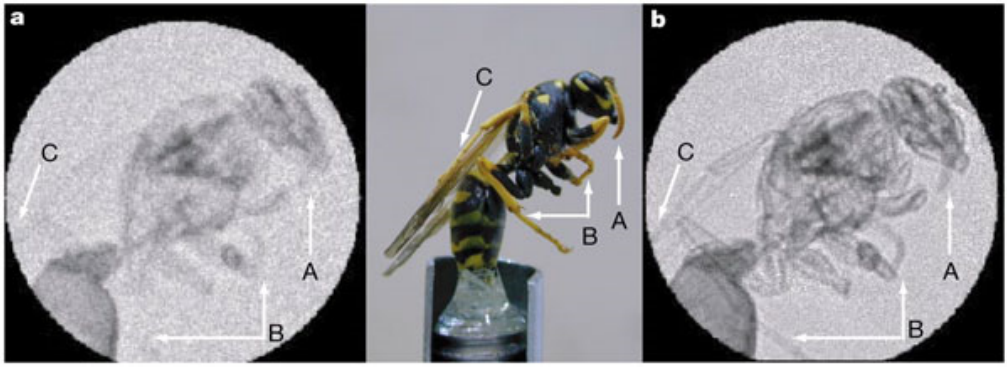

*(a) Neutron attenuation radiograph (b) photograph and (c) phase contrast radiograph of a yellow jacket wasp. [B. E. Allman et al., **Nature** 408 (2000) 158]*

Phase Radiography using Grating Interferometry

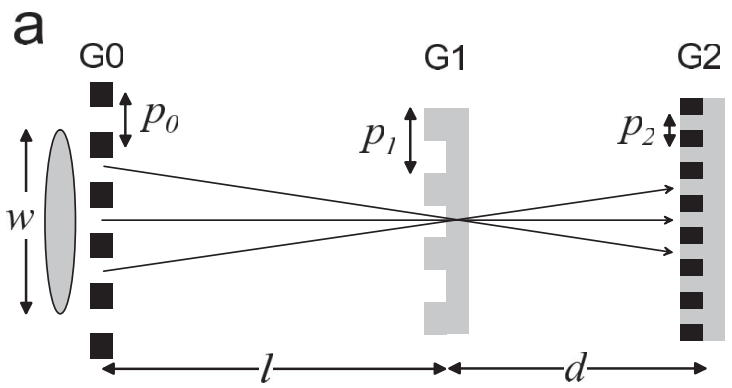

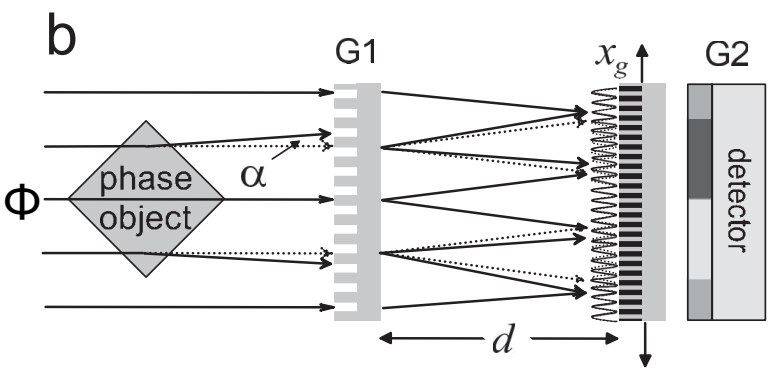

G0: (source) absorption grating, period p_0
G1: phase grating, period p_1
G2: (analyzer) absorption grating, period p_2

*[Pfeiffer et al., **PRL. 96** (2006) 215505]*

- G0 creates array of coherent sources from source *w*
- G1 creates diffraction patterns for each source which overlap if

$$p_0 = p_2 \frac{l}{d}$$

- Diffraction pattern has maximum contrast when *d* is a integer multiple of the Talbot length, L_T

$$L_T = \frac{p_1^2}{\lambda}$$

- Phase object cause distortion of diffraction pattern (or phase shift of incident wave Φ)
- Measure diffraction pattern by translating G2

p_0 ~ 1 mm, p_1 ~ 10 μm, p_2 ~ 5 μ m, l ~ 5 m, d ~ 20 mm

Magnetic field of a dipole magnet visualized by spin-polarized neutrons

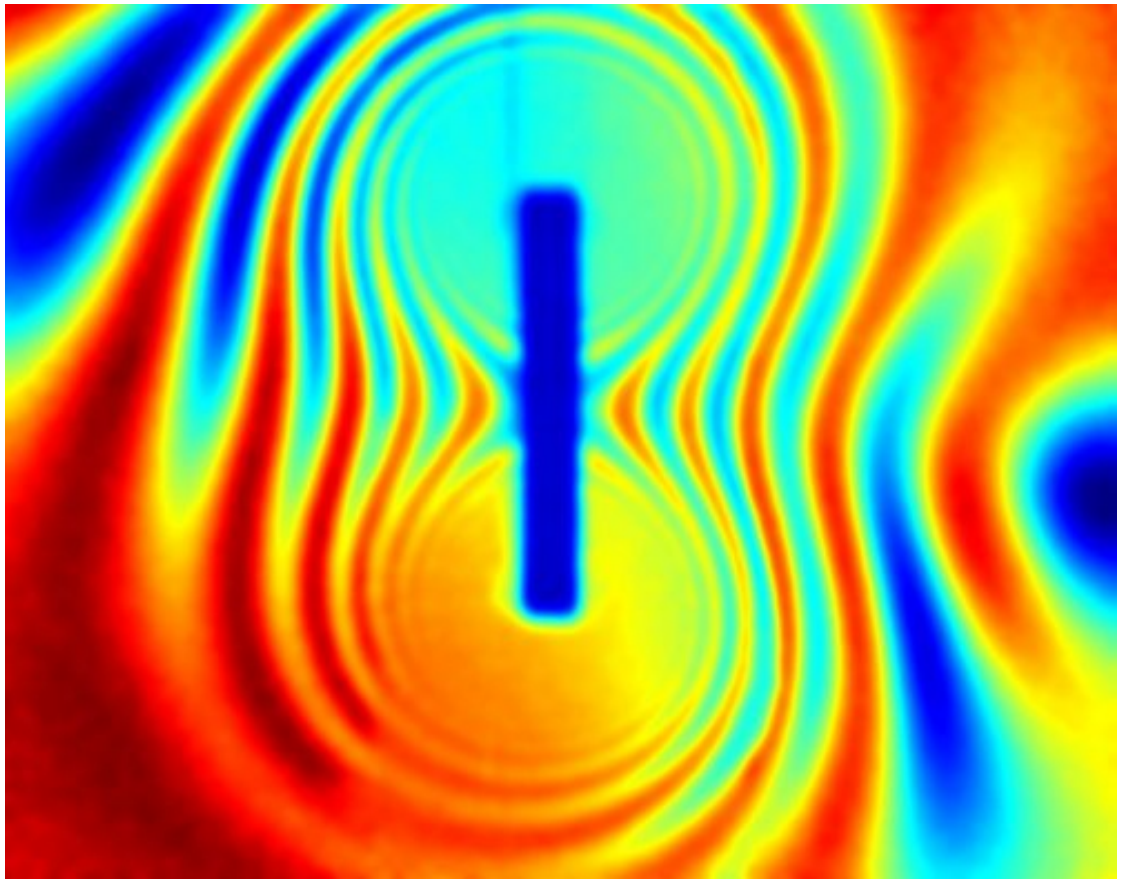

N. Kardjilov et al., http://physicsworld.com/cws/article/news/33694

Stroboscopic imaging

- Makes a cyclically moving object appear to be slow moving
- Pulsed sources are by definition stroboscopic neutron sources

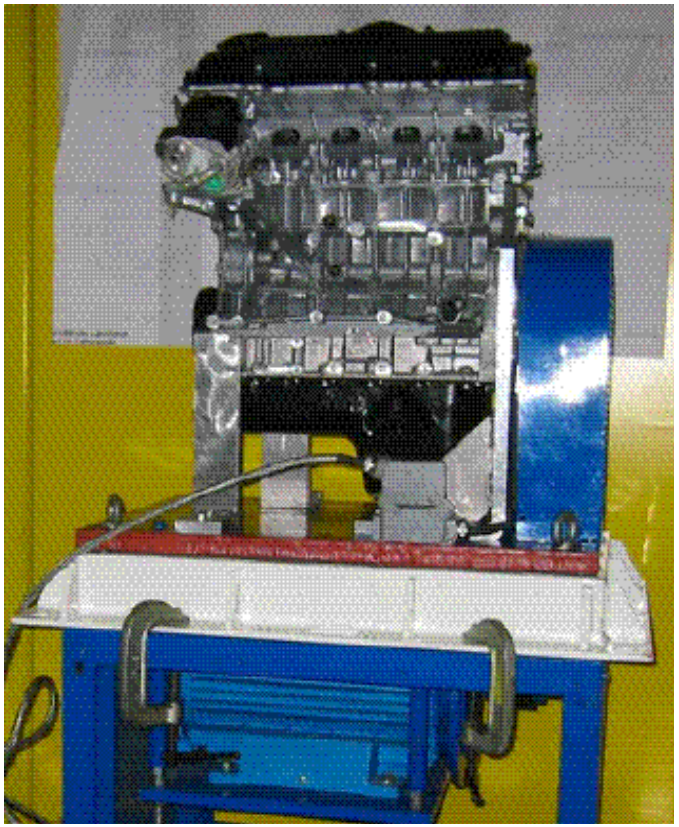

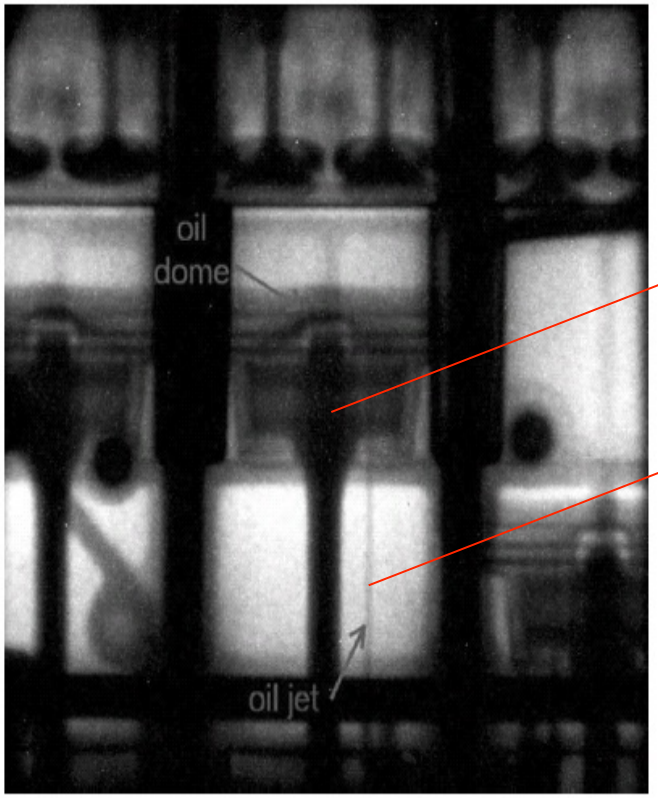

Oil spreading into bottom of piston

Oil jet ejected into bottom of piston

Stroboscopic imaging: 150 exposures, 200 ms each, 24 cm x 24 cm field of view

BMW engine, NEUTROGRAPH, ILL, France

Schillinger et al., NIM A **542** (2005) 142.

Applications at a glance

- Archeology
- Bio-medical
- Botany
- Contraband
- Cultural Heritage
- Energy
- Engineering/Materials Science
- Forensic Science
- Geology/Earth Sciences
- Homeland Security
- Paleontology
- Quality Assurance

Visualization of water transport in artificial soil sedimentation (20 s frame, 25 x 25 cm^2)

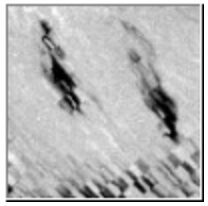

http://neutra.web.psi.ch/gallery/animations.html

Radiography of a dry monkey skull

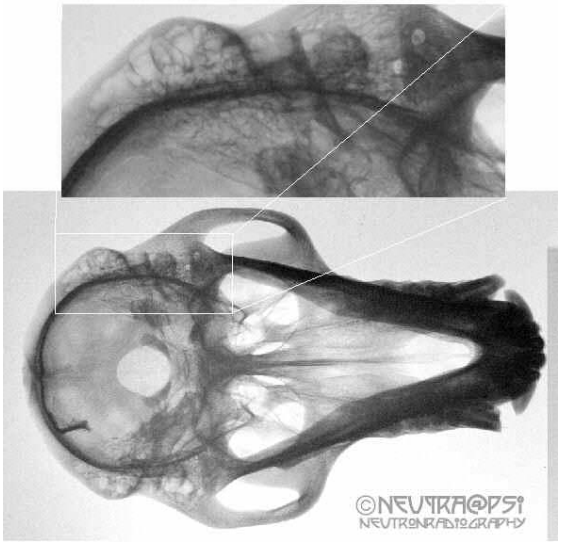

http://neutra.web.psi.ch/gallery/biological.html

Materials Research, Energy and Engineering Applications

A unique inside look of turbine blades produced by additive manufacturing

Advanced materials and processes March 2013 Journal Cover showing a photograph (left), a neutron radiograph (center) and a sliced computed tomography (right) of the Morris Technologies turbine blade.

Scientific Achievement

Non destructive analysis of turbine blades produced by additive manufacturing reveals inside surface roughness and other printing characteristics

Significance and Impact

Neutron computed tomography provides important mapping of the finished product.

Research Details

- **Comparison of engineering drawing and neutron computed tomography is ongoing**
- **Efforts are focused in combining neutron computed tomography with residual strain to gain information on additive manufacturing processes**
- **Surface roughness data may be fed back to Finite Element Analysis computation studies to determine the effect in air flow using the turbine**

T. Watkins, H. Bilheux, K. An, A. Payzant, R. Dehoff, C. Duty, W. Peter, C. Blue, C. Brice, AM&P, 171 23 2

MORRIS TECHNOLOGIES
Precision. Innovation. Expertise.

Work performed at ORNL's High Flux Isotope Reactor CG-1D and Spallation Neutron Source VULCAN beamlines was supported by Scientific User Facilities Division, Office of Basic Energy Sciences, US Department of Energy.

Fabrication tolerance studies comparing CAD drawing to neutron computed tomography

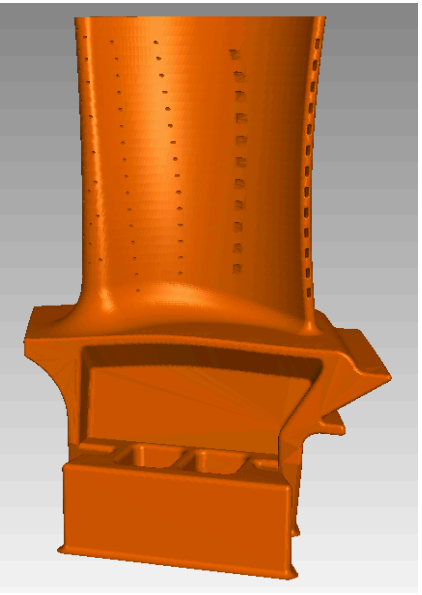

Engineering drawing

+

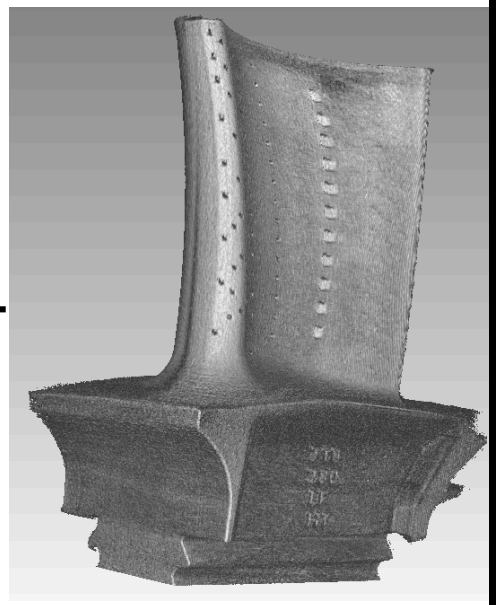

Neutron CT

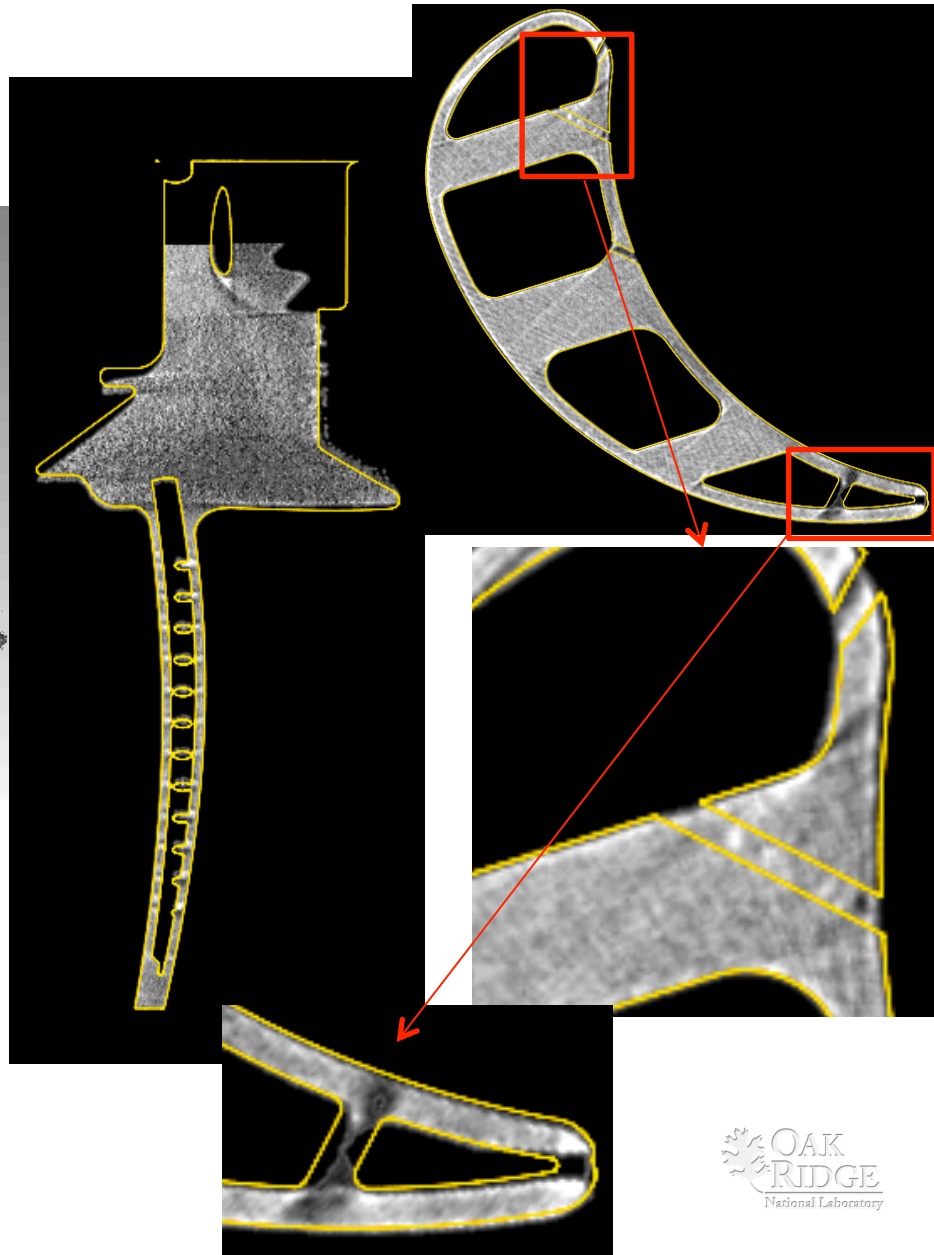

In orange/yellow: AUTOCAD outline
In gray: neutron data

OAK RIDGE National Laboratory

Comparison of Li Distribution as a function of depth of battery

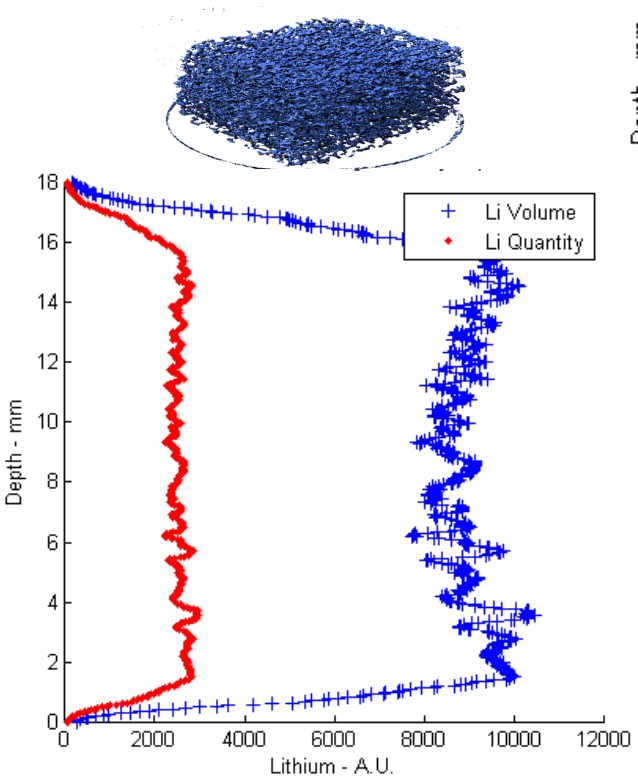

Control

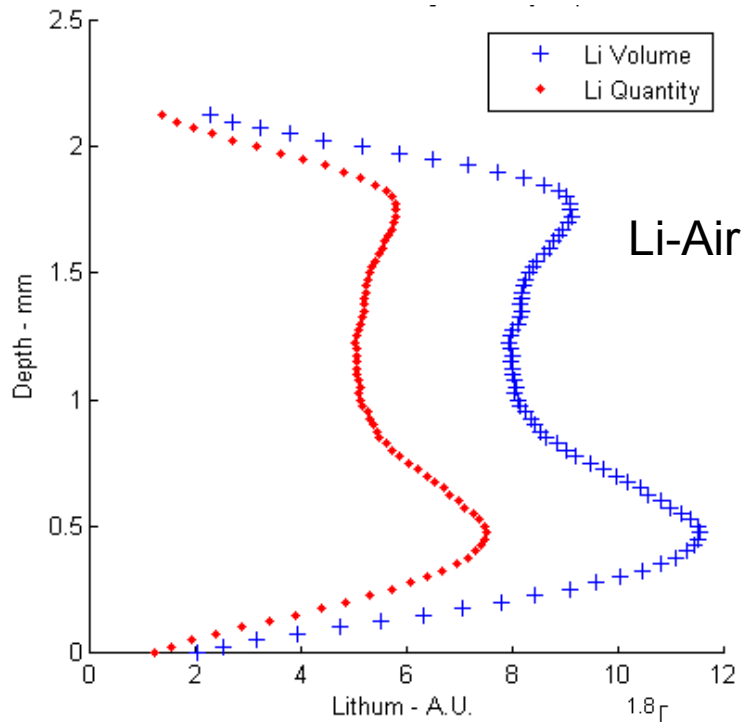

Li-Air (no catalyst)

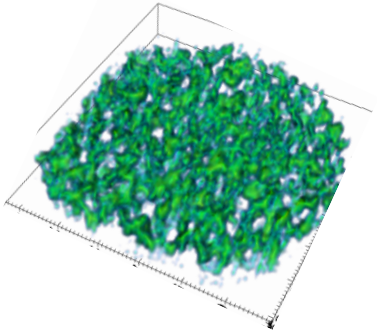

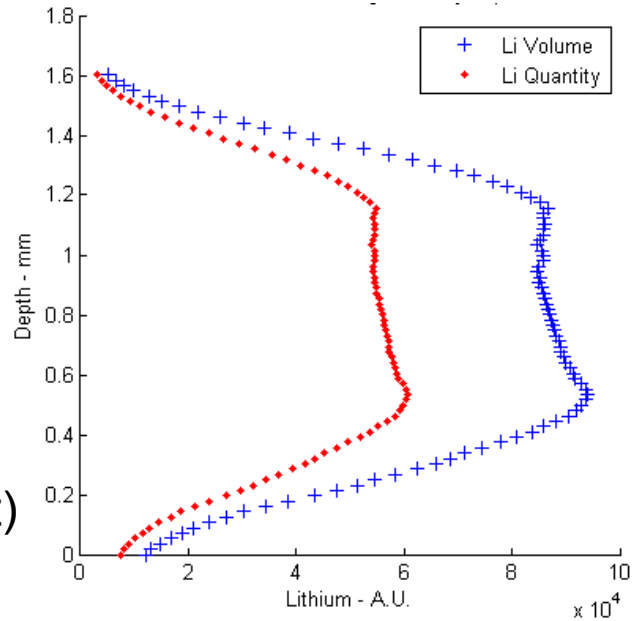

Li-Air (with catalyst)

Nanda et al., Journal of Physical Chemistry C, 2012.

Neutron Imaging Provides the Basis for Developing Models

Non-uniform lithium distribution may limit rechargeability

Neutron image
Li- air cathode

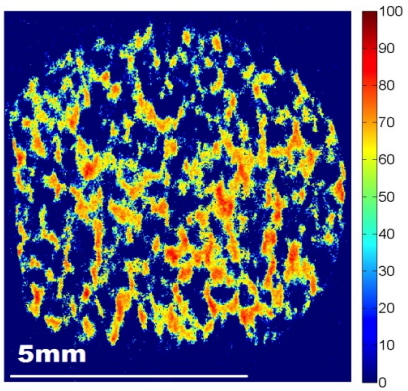

3D model
Li-air cathode

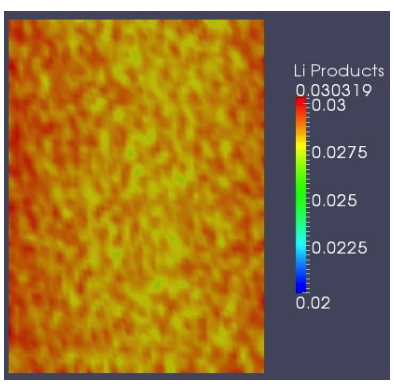

- **Reaction phase 3 dimensional modeling was used to predict results and compare with measurements**
- **Spatiotemporal reaction phase three-dimensional modeling of the electrodes also predicted a non-uniform lithium product distribution, confirming the neutron imaging result.**
- **Need to match resolution of neutron imaging capabilities to further improve feedback to modeling tools**

THE JOURNAL OF PHYSICAL CHEMISTRY C
Article
pubs.acs.org/JPCC

Anomalous Discharge Product Distribution in Lithium-Air Cathodes

Jagjit Nanda,*,† Hassina Bilheux,*,‡ Sophie Voisin,‡ Gabriel M. Veith,† Richard Archibald,§ Lakeisha Walker,‡ Srikanth Allu,§ Nancy J. Dudney,† and Sreekanth Pannala*,§

†Materials Science and Technology Division, ‡Neutron Scattering Science Division, and §Computer Science and Mathematics Division, Oak Ridge National Laboratory, Oak Ridge, Tennessee 37831, United States

OAK RIDGE National Laboratory

Neutron Computed Tomography Characterizes Particulate Properties During Regeneration

Diesel particulate filters (DPF) clean exhaust and reduce pollution

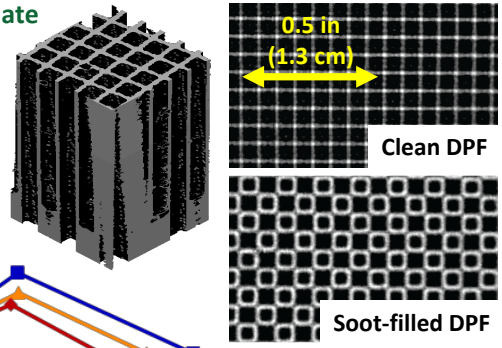

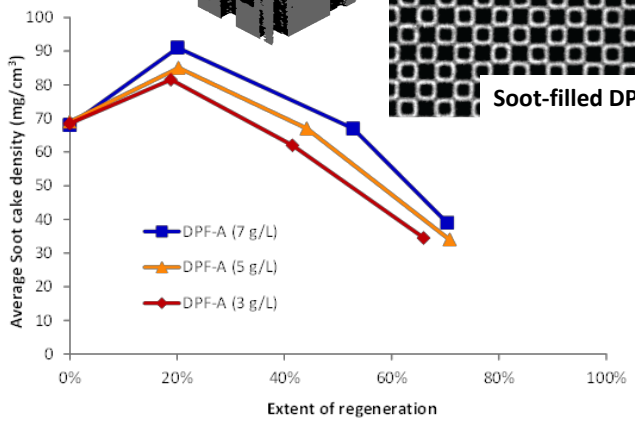

DPFs collect soot during engine operation, leading to soot cake. During regeneration soot cake properties change significantly as identified in neutron imaging campaign.

Work performed at the High Flux Isotope Reactor Imaging (CG1D) beamline was supported by Scientific User Facilities Division, Office of Basic Energy Sciences, US Department of Energy.

T. J. Toops, H. Bilheux, S. Voisin, J. Gregor, L. Walker, A. Strzelec, C. E. A. Finney, J. A. Pihl, Nuclear Instruments and Methods in Physics Research Section A 729 (2013) 581-588.

T. J. Toops, J. A. Pihl, C. E. A. Finney, J. Gregor, H. Bilheux, Emission Control Science and Technology 1:1 (2015) 24-31.

Scientific Achievement

Employed neutron tomography to measure the properties of soot cake layer thickness and subsequently density during a sequential regeneration. Identified key parameters that will aid understanding of the fuel-consuming regeneration process.

Significance and Impact

Understanding the regeneration progression of DPFs is important in improving the efficiency of the process and to understand the correlation between pressure drop and soot level. The results from this work can directly provide model parameters to industry so they can better predict the level soot/ particulate in the DPFs.

Research Details

- DPFs were filled to different levels (3, 5 and 7 g/L) using diesel engine
- Full DPFs analyzed with neutron tomography to determine the soot cake thickness and packing density
- Soot cake density, thickness and axial profile measured during sequential regeneration
- Highest soot cake density observed during initial 20% regeneration; layer then loses density, porosity increases and channels open up
- Different soot loading displayed same behavior during regeneration

Neutron Tomography of Industry-Provided Cooler Tube Sections

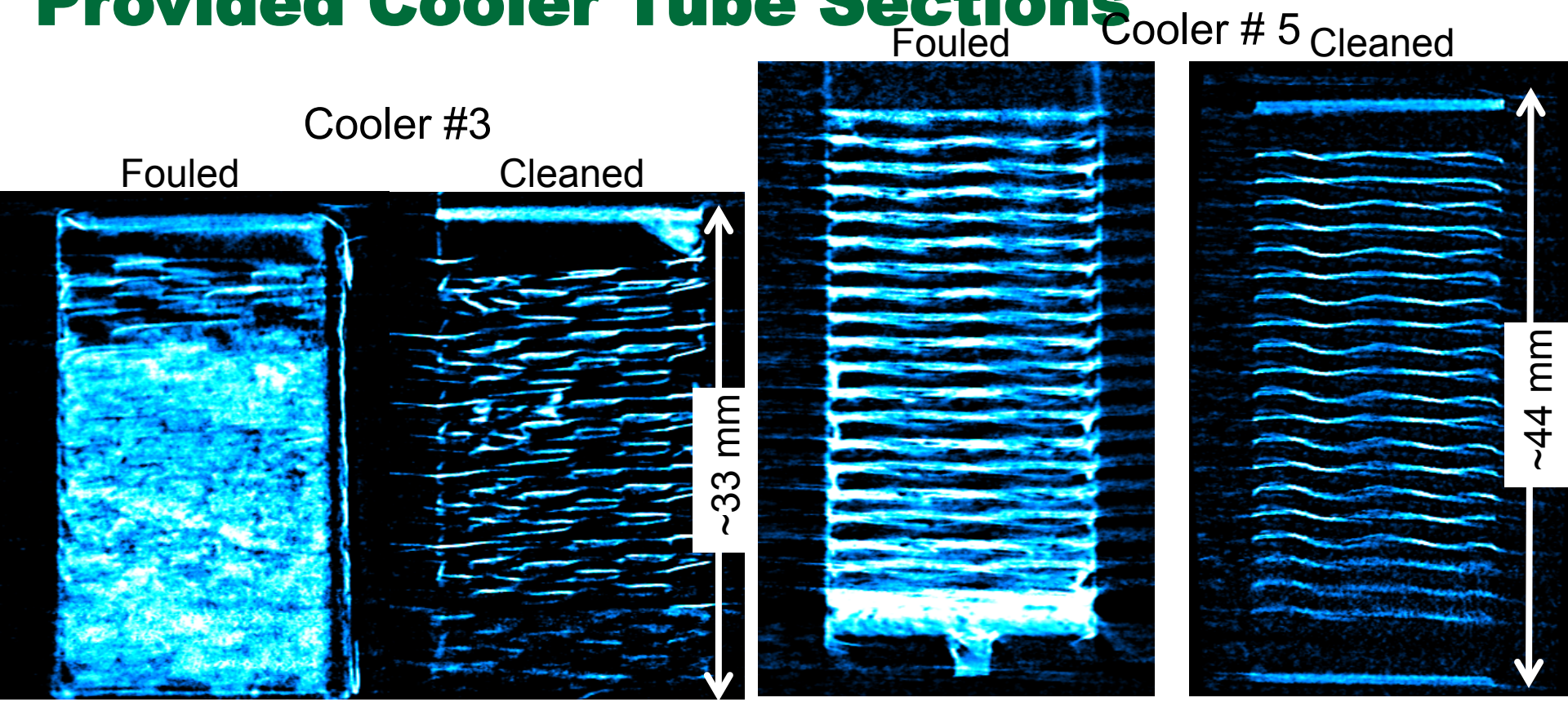

- **Slices can be collected along any plane through the cooler.**
- **The resolution was not high enough to measure thickness directly but we can still gather useful information about the deposit location relative to the heat exchanger geometry.**

M. Lance, S. Sluder, H. Bilheux, S. Voisin, J. Gregor, J. –C. Bilheux

Ancient Craft Skills meet Modern Characterization

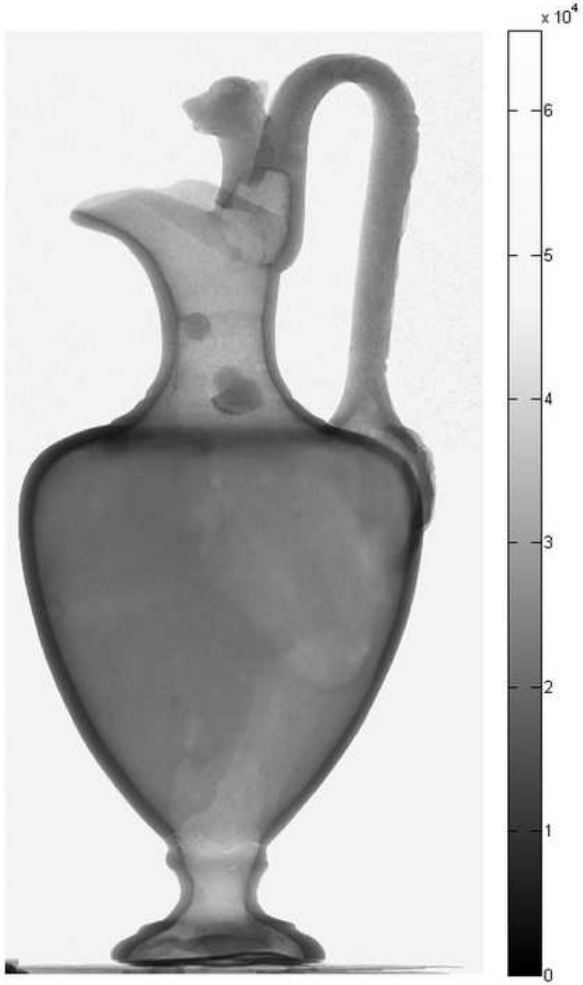

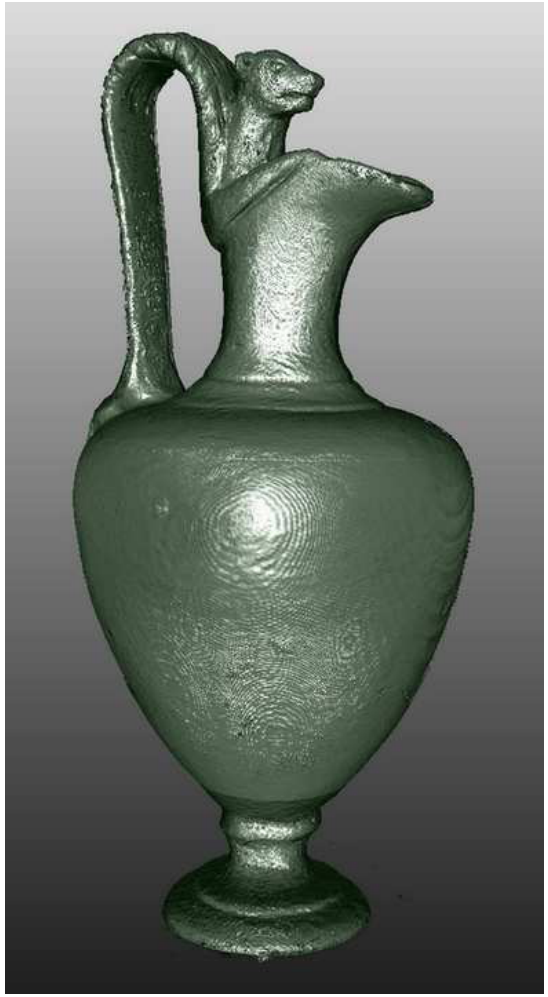

K. Ryzewski (PI), S. Herringer, H. Z. Bilheux, J.-C. Bilheux, B. Sheldon

OAK RIDGE National Laboratory

Ancient Craft Skills meet Modern Characterization

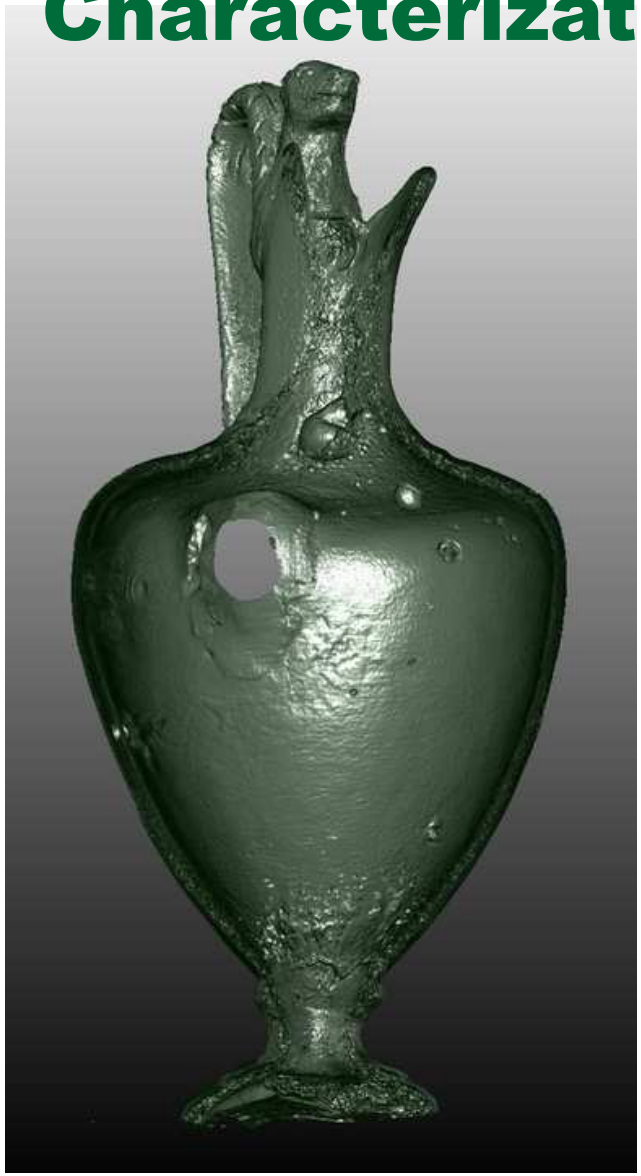

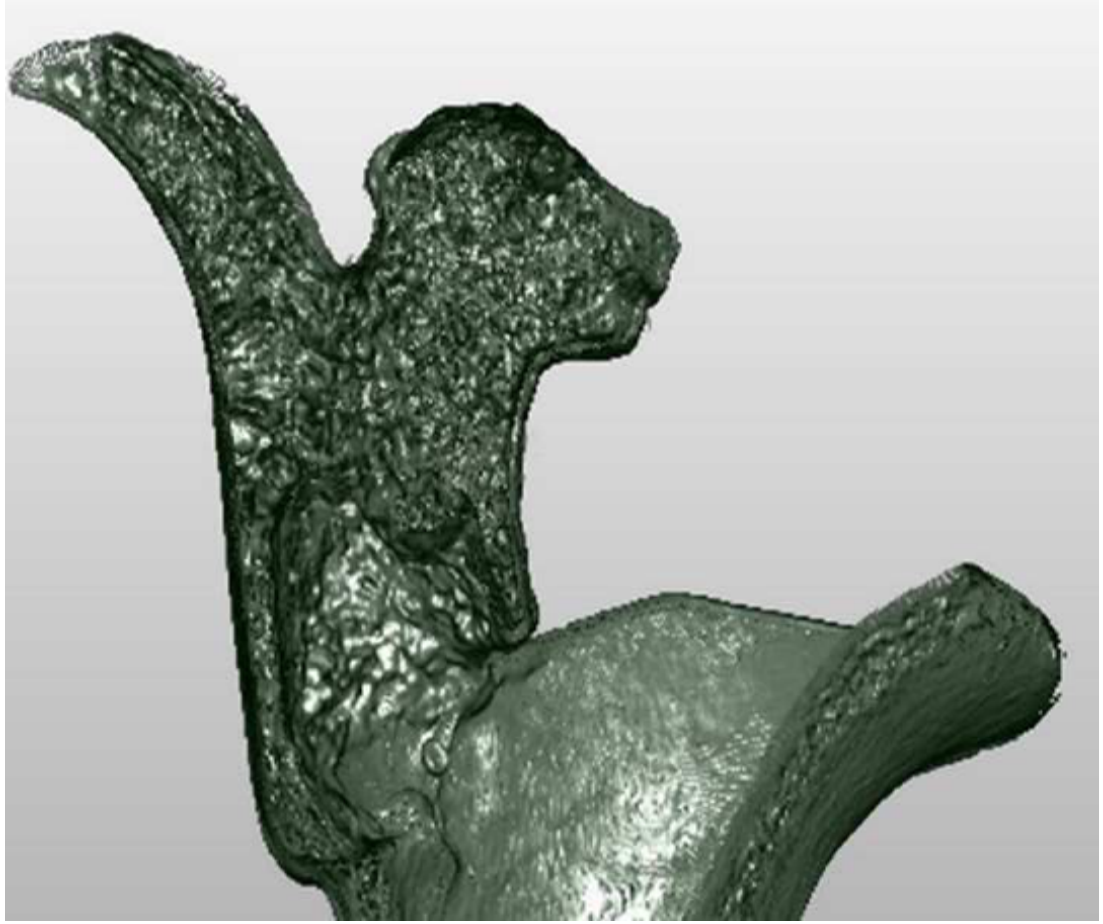

K. Ryzewski (PI), S. Herringer, H. Z. Bilheux, J.-C. Bilheux, B. Sheldon

OAK RIDGE National Laboratory

Biological and Environmental Applications

Rapid Imbibition of Water in Fractures within Unsaturated Sedimentary Rock

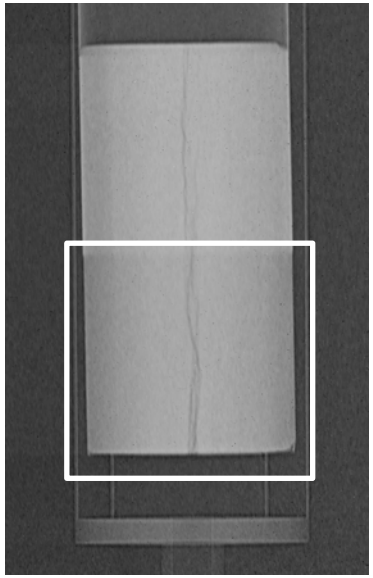

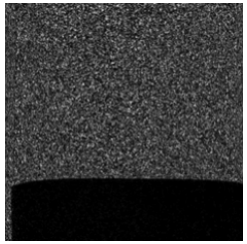

0 sec

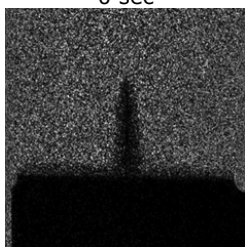

0.5 sec

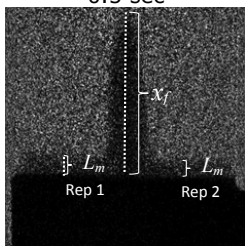

1.4 sec

Time sequence of neutron radiographs showing the rapid uptake of water into a longitudinal, air-filled fracture zone in Berea sandstone (~50 mD). FOV is ~28 x 28 mm^2.

Work performed at the High Flux Isotope Reactor Imaging beam line (CG1D) was supported by the Scientific User Facilities Division, Office of Basic Energy Sciences, U.S. Department of Energy.

Scientific Achievement

Spontaneous imbibition of liquids into gas-filled fractures in variably-saturated porous media is important in a variety of engineering and geological contexts. Dynamic neutron radiography was applied to directly quantify this phenomenon in terms of sorptivity and dispersion coefficients.

Significance and Impact

The theory derived describes rapid early-time water movement into air-filled fractures in sedimentary rock. Both theory and observations indicate that fractures significantly increase spontaneous imbibition and dispersion of the wetting front in unsaturated sedimentary rocks. Capillary action appears to be supplemented by surface spreading on rough fracture faces. The findings can be applied in modeling hydraulic fracturing.

Research Details

Imbibition into unsaturated Berea sandstone cores was controlled with a Mariotte bottle setup. Images were collected using dynamic neutron radiography and analyzed using ImageJ.

Cheng C. -L., Perfect E., Donnelly B., Bilheux H. Z., Tremsin A. S., McKay L. D., DiStefano V. H., Cai J. C., Santodonato L. J., Rapid imbibition of water in fractures within unsaturated sedimentary rock. 2015. Advances in Water Resources, Volume 77, Pages 82–89 <http://dx.doi.org/10.1016/j.advwatres.2015.01.010>

OAK RIDGE National Laboratory

Imaging and modeling of fluid flow in non-homogeneous porous media

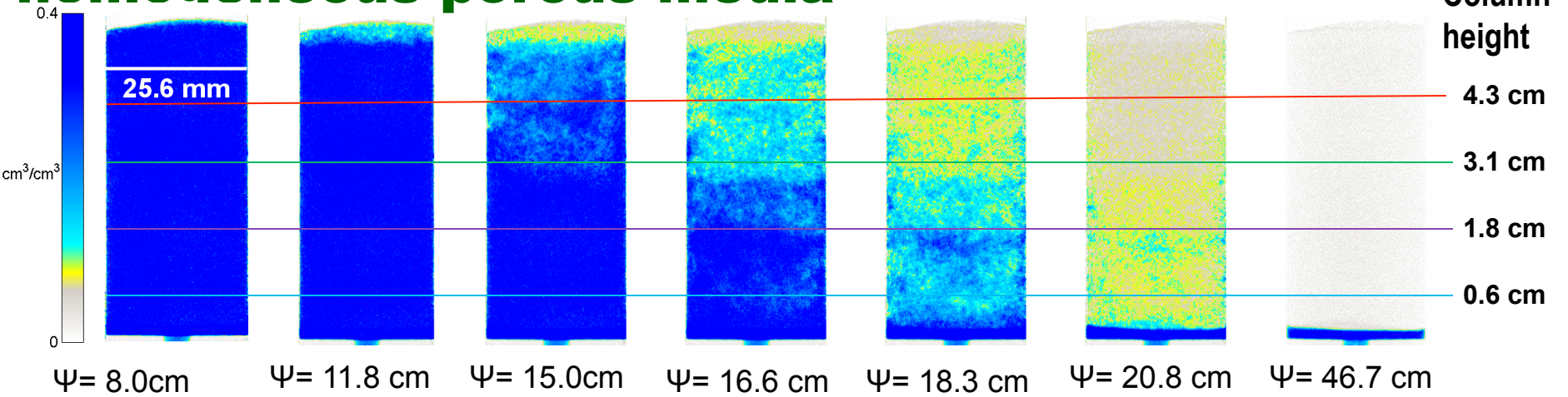

(Blue: water)

Flint Sand Drying Process (HFIR /CG1-D)

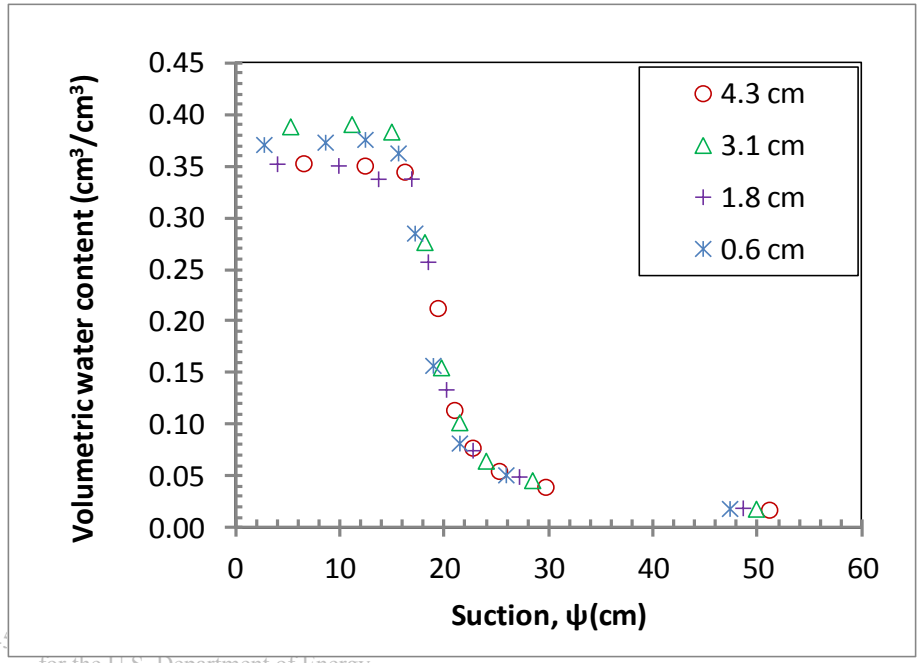

- Measured point functions varied with column height
- Heterogeneity due to packing procedure
- Input parameters for numerical model

Cheng, C.-L. et al., Soil Sci. Soc. Am. J. 76:1184–1191 doi:10.2136/sssaj2011.0313
Kang, M. et al., NIM A, accepted

Point Water Retention Function: hanging water column

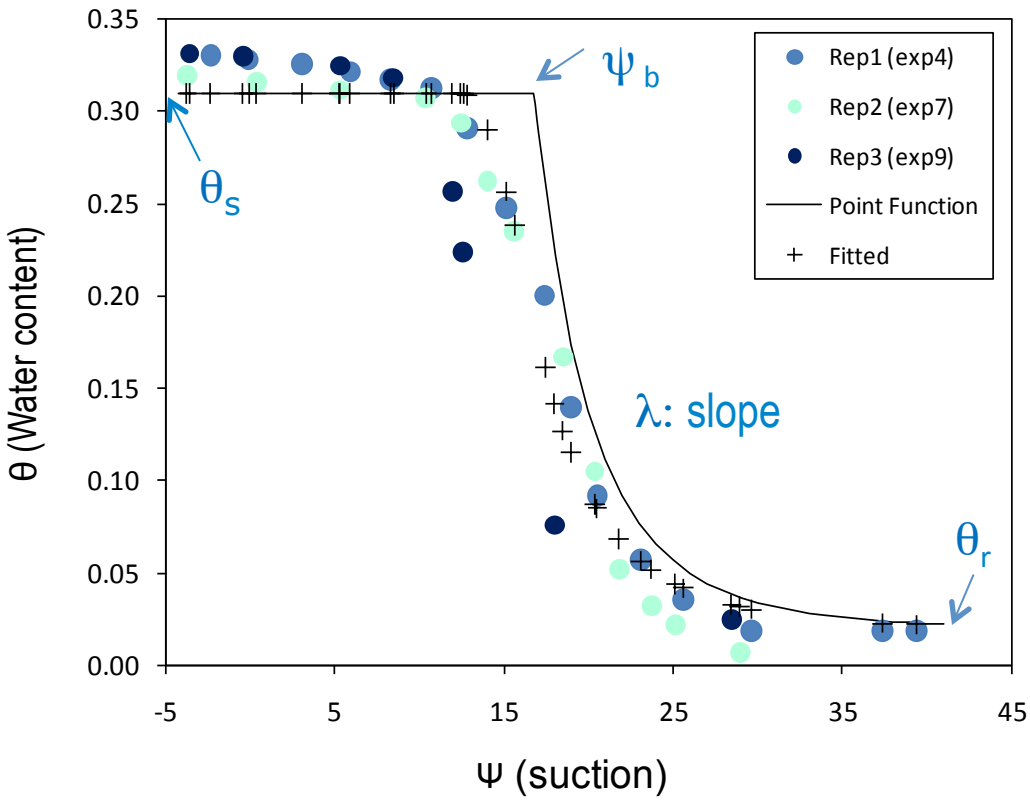

Brooks and Corey Parameters

- θ_r = residual water content (cm^3cm^{-3})
- θ_s = saturated water content (cm^3cm^{-3})
- ψ_b = air entry value (cm)
- λ = pore-size distribution index

➢ Point water retention function is extracted from the average water retention curve determined by hanging water column using TrueCell inverse modeling procedure

Neutron Radiography of Roots at CG1-D

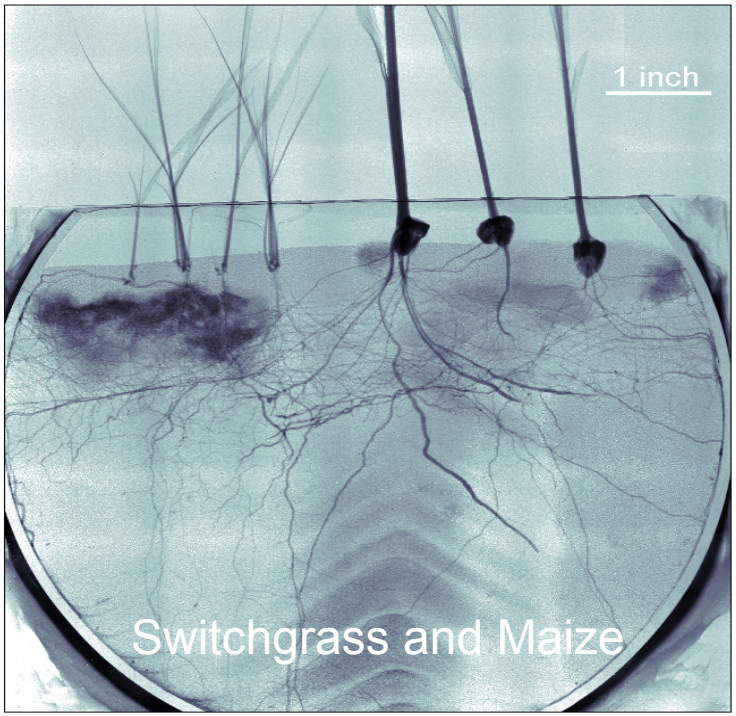

- Water injected into root zone at base
- Unidentified endophyte (symbiotic) or decomposer fungi visible near roots of switchgrass (left), revealing substantial hydration of the rhizosphere
- Both fine and coarse roots are readily visible

Water Uptake by Roots and Stem

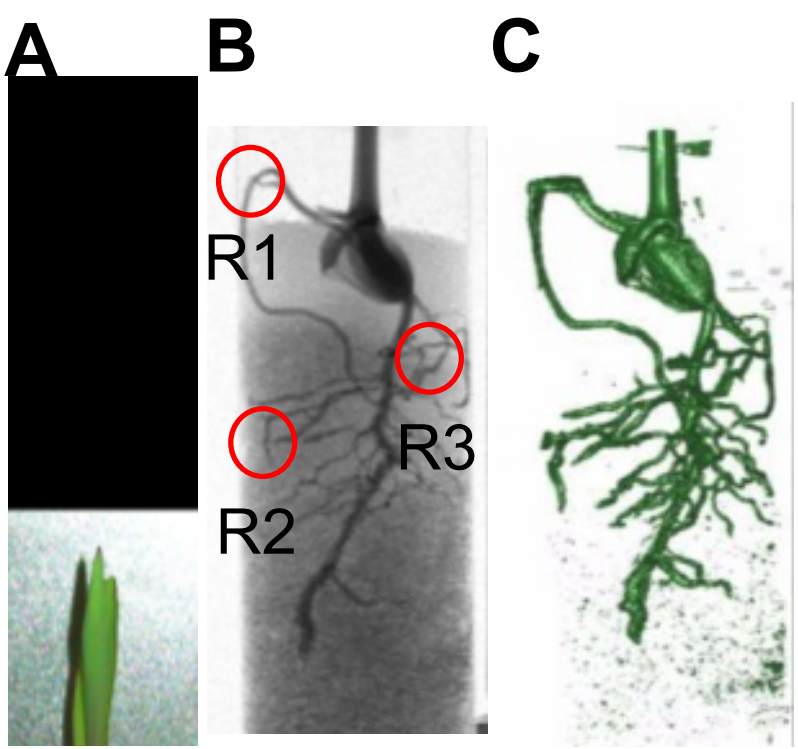

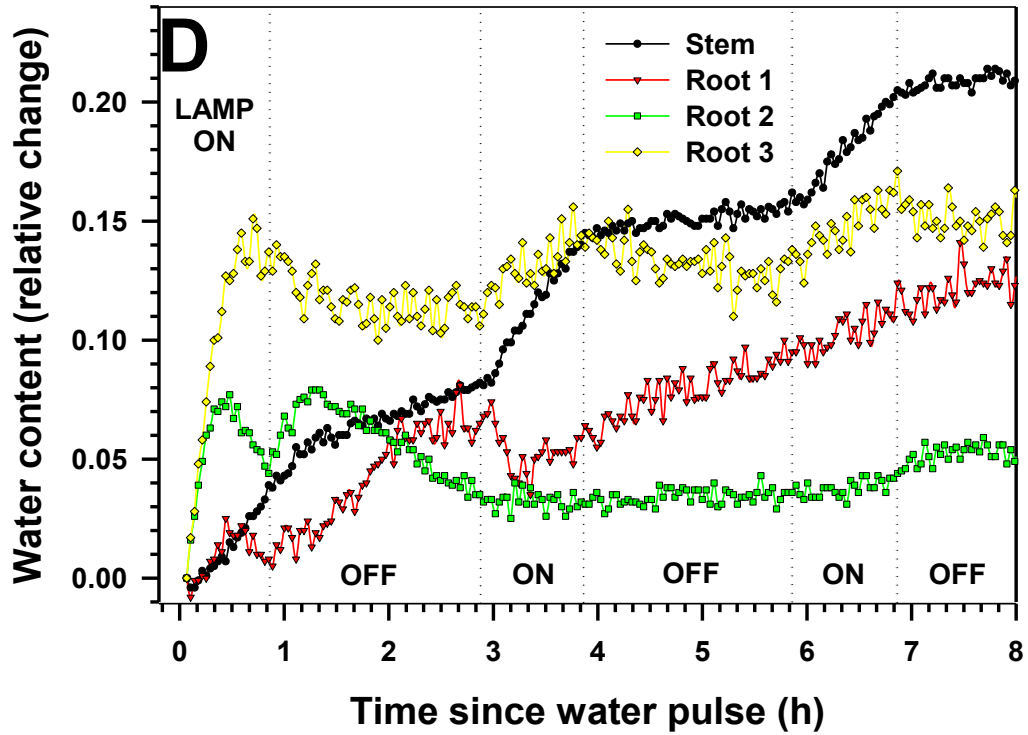

10-d old maize seedling (A) aluminum sample chamber; (B) neutron radiograph at ~70 μm pixel resolution illustrating roots distribution (0.2-1.6 mm); C) 3D tomographic reconstruction; (D) Timing of water uptake by plant components highlighted in (B) illustrating impact of solar radiation on rate of water flux in stem and ~0.5 mm first and second order roots.

- This study provides direct evidence for root-mediated hydraulic redistribution of soil water to rehydrate drier roots

A novel approach to determine post-mortem interval using neutron radiography

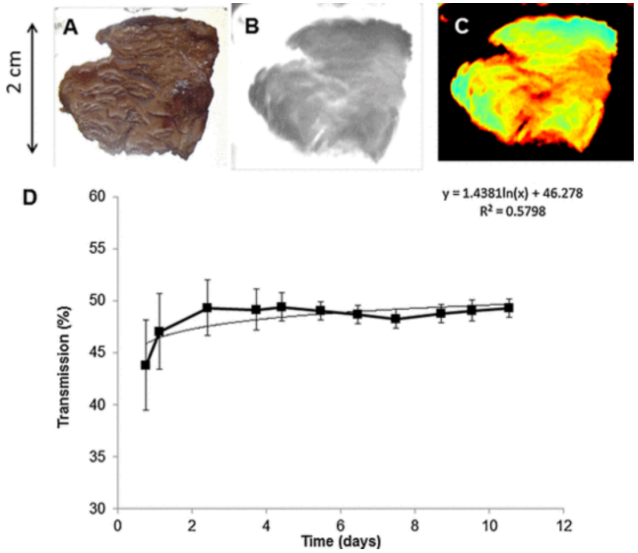

(A) Photograph, (B) gray scale and color enhanced (C) neutron radiograph of a 2 cm × 2 cm × 1 mm thick skeletal muscle tissue. (D) Neutron transmission as a function of time of skeletal muscle tissues under controlled conditions with natural logarithm fit.

H. Z. Bilheux, M. Cekanova, A. A. Vass, T. L. Nichols, J. C. Bilheux, V. Finochiarro, **Forensic Science International**, doi:10.1016/j.forsciint.2015.02.017 (March 2015)

Work performed at ORNL's High Flux Isotope Reactor CG-1D and Spallation Neutron Source VULCAN beamlines was supported by Scientific User Facilities Division, Office of Basic Energy Sciences, US Department of Energy. Part of this research sponsored by NIJ.

Scientific Achievement

PMI was objectively estimated by measuring changes in neutron transmission correlated with H content variation in decaying tissues.

Significance and Impact

- One of the most difficult challenges in forensic research for criminal justice investigations is to objectively determine post-mortem interval (PMI).
- The estimation of PMI is often a critical piece of information for forensic sciences.
- Most PMI techniques rely on gross observational changes of cadavers that are subjective to the forensic anthropologist.

Research Details

- Tissues exposed to controlled (laboratory settings) and uncontrolled (University of Tennessee Anthropology Research Facility) environmental conditions.
- Neutron radiographs were compared to histology data to assess the decomposition stage
- Over a period of 10 days, changes in neutron transmission through lung and muscle were found to be higher than bone by 8.3%, 7.0%, and 2.0%, respectively.

U.S. DEPARTMENT OF ENERGY | Office of Science

NIJ | National Institute of Justice
STRENGTHEN SCIENCE. ADVANCE JUSTICE.

OAK RIDGE National Laboratory

NEUTRON SCIENCES
Spallation Neutron Source • High Flux Isotope Reactor

Muscle June 2012

A

B

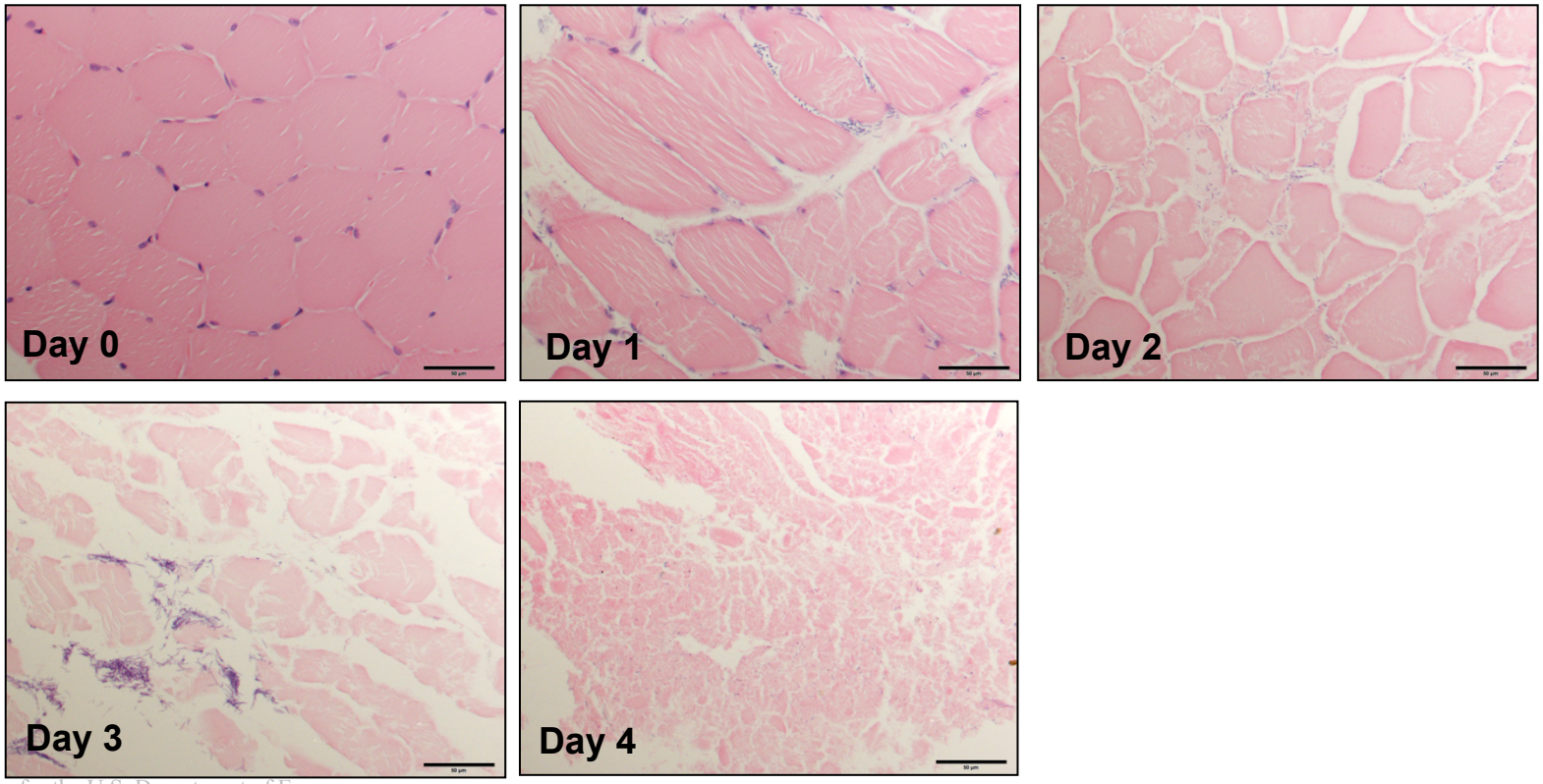

for the U.S. Department of Energy
OAK RIDGE National Laboratory

Imaging at the Spallation Neutron Source: the future VENUS beamline

VENUS at the Spallation Neutron Source: a unique tool for basic and applied research

$$I(\lambda) = I_0(\lambda)e^{-\mu(\lambda)x} \qquad \mu(\lambda) = \sigma_t(\lambda)\frac{\rho N_A}{M}$$

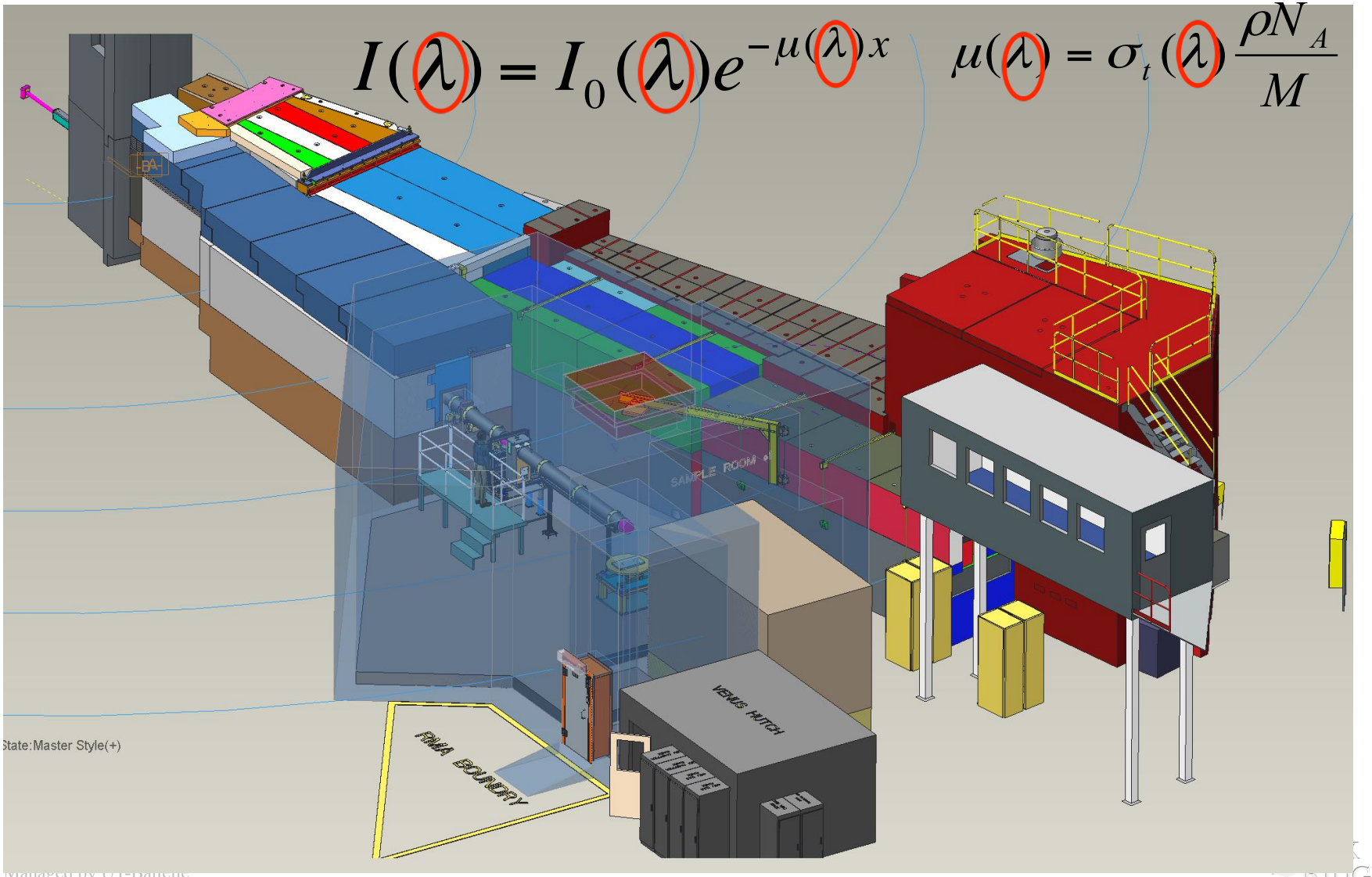

Managed by UT-Battelle
for the U.S. Department of Energy

Bragg's law in transmission mode

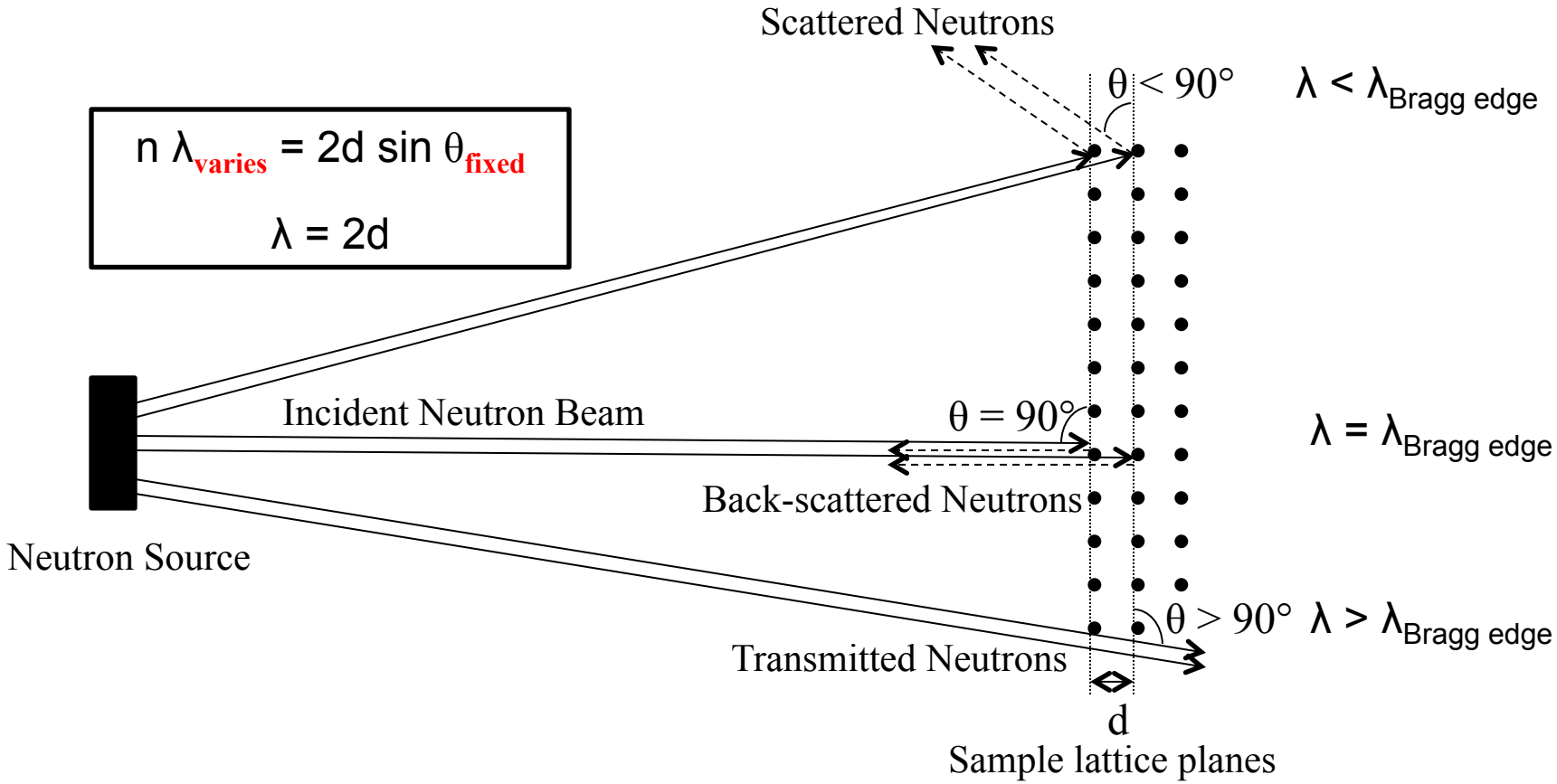

(Top) For a specific neutron wavelength, λ, shorter than the Bragg edge wavelength, $\lambda_{\text{Bragg edge}}$, the incident neutron beam enters the crystalline lattice with $\theta < 90°$ and is scattered with a deviation of 2θ. (Center) The lattice planes are aligned with the incident neutron, i.e. $\theta = 90°$, which back-scattered towards the neutron source. (Bottom) For a neutron wavelength longer than the Bragg edge wavelength, there is no diffraction and the neutron beam can transmit. In this figure, d is the distance between lattice planes and θ is the scattering angle.

Energy-resolved neutron radiograph of crystalline structures

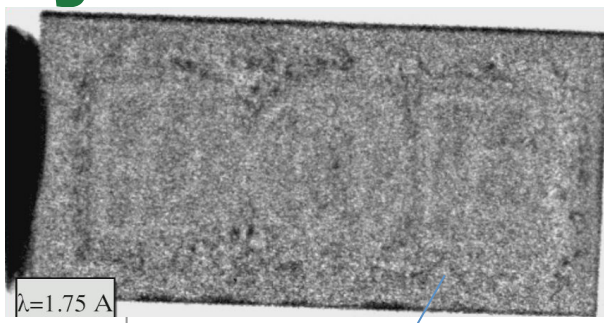

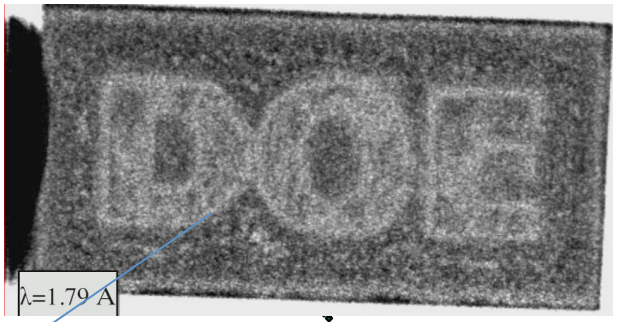

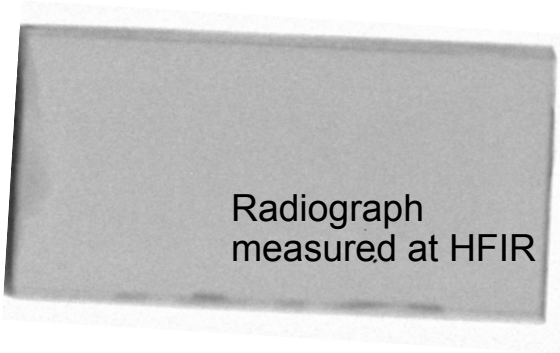

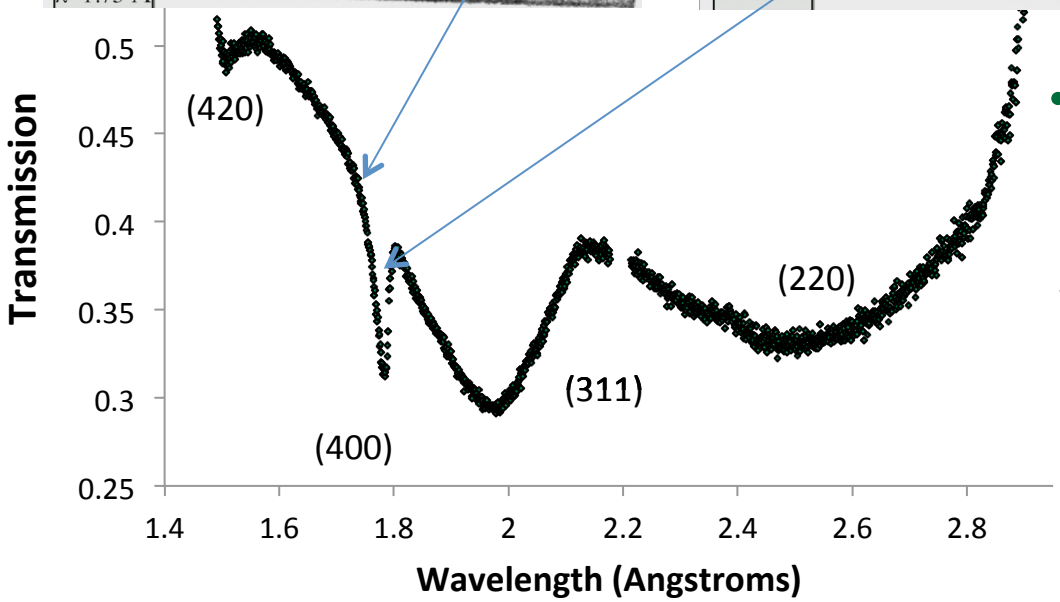

Mapping of Bragg edge and corresponding crystalline orientation in Inconel 718 structures, as identified using Time-Of-Flight imaging. "DOE" letters are polycrystalline structures and the surroundings are textured.

- **Demonstrated that SNS's unique pulsed source enables mapping of crystalline planes in complicated geometries including textured samples**
  - **Sample was Inconel 738 made by additive manufacturing**
  - **Micro-channel plate detector (MCP) temporarily installed at VULCAN**
  - **Time-binned (5.2μs) data collection.**

Work performed at ORNL's Spallation Neutron Source VULCAN beamlines was supported by Scientific User Facilities Division, Office of Basic Energy Sciences, US Department of Energy.

OAK RIDGE National Laboratory

Mapping of crystalline structures

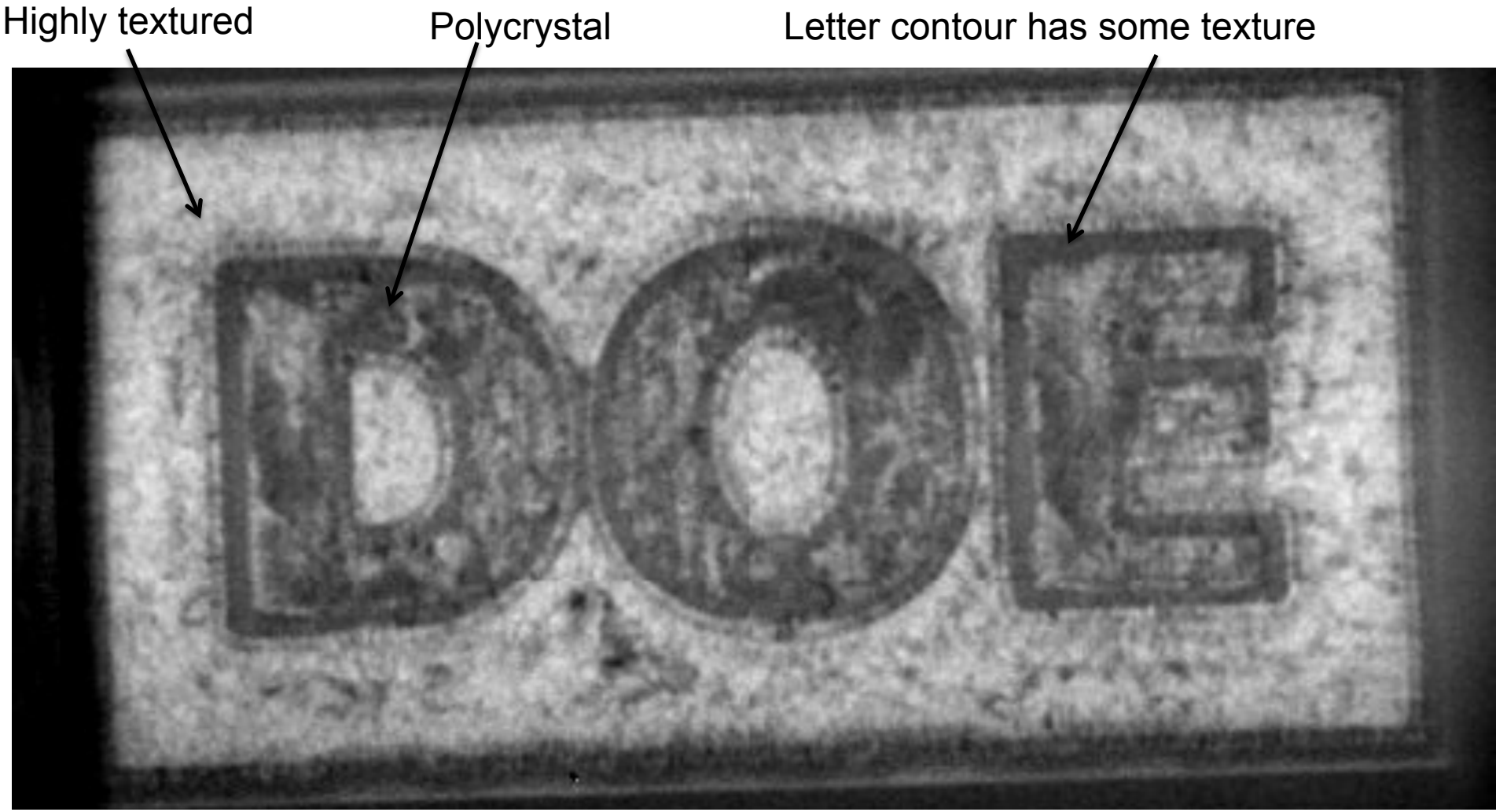

R. R. Dehoff,, M. M. Kirka,, W. J. Sames,, H.Bilheux, A. S. Tremsin, L. E. Lowe, and S. S.Babu,,. "Site specific control of crystallographic grain orientation through electron beam additive manufacturing." *Materials Science and Technology* 2015

DOI: 10.1179/1743284714Y.0000000734

Managed by UT-Battelle
for the U.S. Department of Energy

Acknowledgments

- ORNL contributions from: Lou Santodonato, Ke An, Jean Bilheux, Barton Bailey, Ken Herwig, Scott Keener, Larry Davis, Irina Popova, Ryan Dehoff, Mike Kirka, Lindsay Kolbus, Todd Toops, Charles Finney, Eric Nafgizer, Derek Splitter, Jagjit Nanda
- Anton Tremsin, University of CA - Berkeley
- Ed Perfect, Jen Gregor, University of TN – Knoxville
- Chu-Lin Cheng, University of Texas – Pan America/Rio Grande Valley
- Hui Zhou, Hong Kong Science Park
- Industry collaborators
- US DOE Scientific User Facilities Division, Office of Basic Energy Sciences, US Department of Energy
- US DOE Energy Efficiency and Renewable Energy, Additive Manufacturing Office, US Department of Energy

Thank you
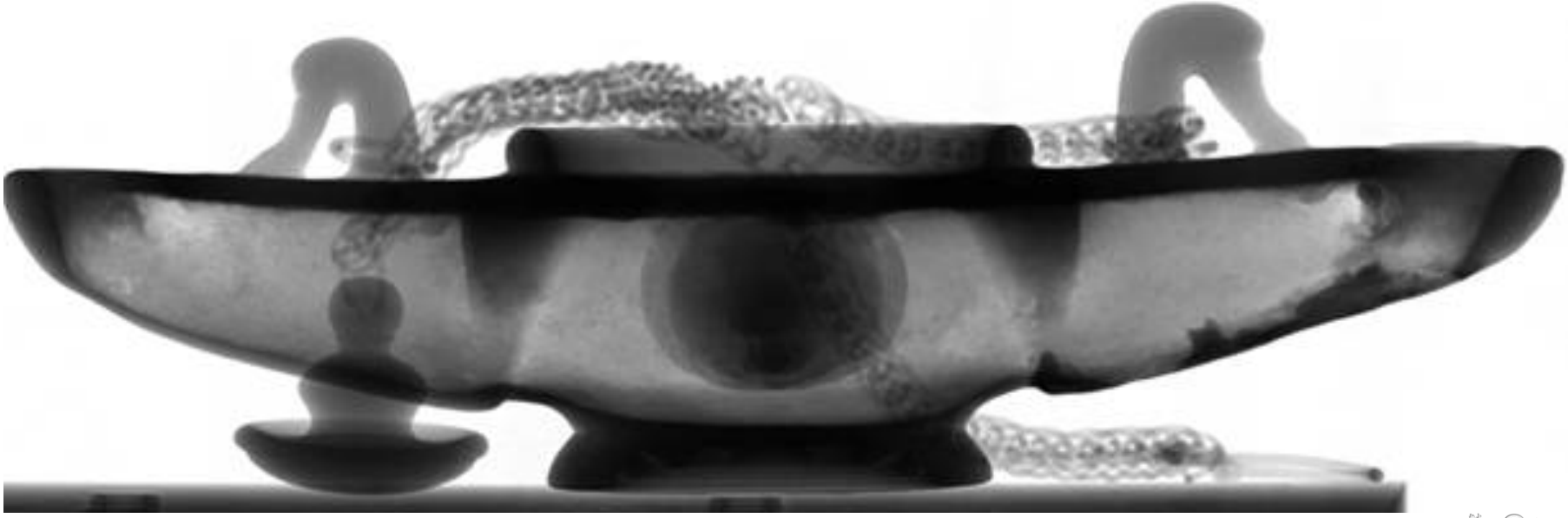
Courtesy of
Krysta Ryzewski, Wayne University
Susan Herringer, Brian Sheldon,
Brown University